

Non-Linear Proportional Integral Derivative Controller for Active Quarter Car Suspension System



Kenean Alemu Miretie

A Thesis Submitted to

Department of Electrical Power and Control Engineering

School of Electrical Engineering and Computing

Presented in Partial Fulfillment of the Requirement for the Master of Science
Degree in Electrical Power and Control Engineering (Control Engineering)

Office of Graduate Studies

Adama Science and Technology University

October 2023.

Adama, Ethiopia.

Non-Linear Proportional Integral Derivative Controller for Active Quarter Car Suspension System

Kenean Alemu Miretie

Advisor: Dr. Tefera Terefe

A Thesis Submitted to
The Department of Electrical Power and Control Engineering
School of Electrical Engineering and Computing

Presented in Partial Fulfillment of the Requirement for the Master of Science
Degree in Electrical Power and Control Engineering (Control Engineering)

Office of Graduate Studies
Adama Science and Technology University

October 2023.
Adama, Ethiopia.

DECLARATION

I declare that this thesis entitled “Non Linear Proportional Integral Derivative Controller for Active Quarter Car Suspension System” is my original work and has not been submitted to any university for a similar purpose. The references used in this thesis are duly recognized by proper citations.

Kenean Alemu Miretie

Name of student

Signature

Date

RECOMMENDATION OF ADVISORS/ SUPERVISORS

I the major advisor/supervisor of this thesis, hereby certify that I have closely advised/supervised the student while developing this and read the draft thesis entitled **“Non-Linear Proportional Integral Derivative Controller for Active Quarter Car Suspension System”** prepared under my guidance by **Kenean Alemu Miretie**. Therefore, I recommend the submission of revised version of the thesis to the department following the applicable procedures

Dr. Tefera Terefe

Major Advisor/Supervisor

Signature

Date

APPROVAL SHEET

I, the advisor of the thesis entitled “**Non-Linear Proportional Integral Derivative Controller for Active Quarter Car Suspension System**” developed by **Kenean Alemu Miretie**, hereby certify that the recommendation and suggestions made by the board of examiners are appropriately incorporated into the final version of the thesis.

Dr. Tefera Terefe _____

Major Advisor/Supervisor

Signature

_____ Date

We, the undersigned, members of the Board of Examiners of the thesis by **Kenean Alemu Miretie**. have read and evaluated the thesis “**Non-Linear Proportional Integral Derivative Controller for Active Quarter Car Suspension System**” and examined the candidate during the open defenses. This is, therefore, to certify that the thesis is accepted for partial fulfillment of the requirement of the degree of Master of Science in Electrical Power and Control Engineering, postgraduate in Control Engineering.

Chairperson

Signature

Date

Dr. Beteley Teka _____



October 28, 2023

External Examiner

Signature

Date

Internal Examiner

Signature

Date

Finally, approval and acceptance of the thesis are contingent upon the submission of its final copy to the Office of Postgraduate Studies (OPGS) through the Department Graduate Council (DGC) and School Graduate Committee (SGC).

Department Head

Signature

Date

School Dean

Signature

Date

Office of Postgraduate Studies Dean,

Signature

Date

ACKNOWLEDGMENT

First I would like to thank God for giving me strength and courage to finish my project. Next, I would like to take the opportunity to express our gratitude to respected supervisor Dr. Tefera Terefe for his patience assistance and support. He gave me proper guidance and valuable advices. His comments and guidance helped me in preparing my project report. Finally, I would like to express our gratefulness to the individuals who involved direct or indirectly during the progress of this project.

ABSTRACT

This thesis aims to see what kinds of performance improvements can be achieved using a non-linear proportional integral derivative controller on quarter-car model suspensions for passenger car applications. To construct a control system for a quarter-car model with constant sprung mass, unsprung mass, damping coefficient, and tire stiffness has been created. Control objectives including sprung mass acceleration minimization and dynamic tire compression, as well as suspension travel. Dynamic tire compression is employed as a predictor of handling quality, whereas the sprung mass acceleration is used to indicate ride comfort. The performances of active suspension system with NPID were evaluated by comparing its respective passive suspension system (PSS). To investigate the effects of road profiles and vehicle speeds on ride comfort and road handling performances, three types of road excitation are designed. These are; random (type A, type B and type C) road inputs and predictable two bumps sinusoidal road inputs. For the random, type A (smooth), type B (good surface) and type C (average), road inputs were designed at four operating vehicle speeds (20km/hr, 40 km/hr, 60km/hr and 80 km/hr). The simulated MATLAB signal statics of peak to peak, .The simulated results of active suspension system and passive suspension system at selected vehicle speeds are investigated under selected random road inputs. Non-linear proportional integral derivative control methods is used to control both ride quality for comfort and vehicle handling can be highlighted by developing a mathematical model for a new design suspension system. As illustrated in the simulation, the comparison of active suspension system with non-linear proportional integral derivative controller is done to their respective passive suspension system for all road inputs and the controlled active suspension system improves ride comfort 66.31% and vehicle handling 95.85%. From this research, it can be concluded that the designed non-linear proportional integral derivative controller have excellent performance for a developed dynamic model, improving the ride quality for passenger safety and vehicle handling under different road disturbances and vehicle speed operations.

Key words: *Non –linear proportional integral derivative, hydraulic actuator, quarter car.*

LIST OF ABBREVIATIONS

OSMC	Optimal Sliding Mode Control
H_∞	H-infinity
LQG	Linear quadratic Gaussian
IEEE	Institute of Electrical and Electronics Engineers
PID	Proportional integrator derivative
LQR	Linear quadratic Regulator
DOF	Degree of Freedom
ANFIS	Adaptive sliding back stepping
PSS	Passive Suspension System
ASS	Active Suspension System
GA	Genetic algorithm
PSO	Particle Swarm Optimization
RMS	Root Mean Square
MFFOSMC	Model free fractional-order sliding mode control
IPID	Integral proportional integrator derivative
LQR	Linear quadratic regulator
ISMC	Integral Sliding Mode Control
ISMC	Integral Sliding Mode Control
ECU	Electric Control Unit
NPID	Nonlinear Proportional Integral Derivative
FOSMC	First Order Sliding Mode Control
ASHC	Active Suspension Homogeneous Controller
SM	Sliding Mode

LIST OF SYMBOLS

m^3	cubic meter
m^2	meter per second
kg	kilo gram
KN/m	kilo Newton per meter
KN	Kilo Newton
ρ	rho
δ	Delta

TABLE OF CONTENTS

Contents

DECLARATION	ii
RECOMMENDATION OF ADVISORS/ SUPERVISORS	iii
APPROVAL SHEET	iv
ACKNOWLEDGMENT	v
ABSTRACT	vi
LIST OF ABBREVIATIONS	vii
LIST OF SYMBOLS	viii
CHAPTER ONE	1
1 INTRODUCTION	1
1.1 Statement of Problem	3
1.2 Objectives of the study	4
1.2.1 General objective	4
1.2.2 Specific objective	4
1.3 Scope of the Study	4
1.4 Significant of project	4
1.5 Outline of the Thesis	5
CHAPTER TWO	7
2 LITERATURE REVIEW	7
2.1 Vehicle Dynamics Modeling	8
2.1.1 Passive Suspension System	9
2.1.2 Semi-active Suspension System	10
2.1.3 Active Suspension System	10
2.2 Hydraulic active suspension system	11
2.3 Review of Related Literatures	12
CHAPTER THREE	15
3 METHODOLOGY	15
3.1 Materials	15
3.2 Methodology	16
3.3 Actuator Modeling	17
3.3.1 Hydraulic active suspension system	17

3.4	Car suspension	18
3.5	Vehicle Suspension Model and Measurements	19
3.5	Road Profile	22
3.5.1	Two bump sinusoidal road profile.....	22
3.5.2	Four bump sinusoidal road profile	23
3.6	Controller system design	27
3.6.1	Non Linear PID Controller	27
3.6.2	Guidelines to obtain parameters of NPID controller	29
3.7	Stability Test	30
CHAPTER FOUR		33
4	RESULTS AND DISCUSSION	33
4.1	Simulation for validation of the vehicle suspension model	34
4.1.1	Performance analysis on the suspension system with NPID controller.....	35
4.2	Two pump sinusoidal road input disturbance.....	35
4.3	Four pump sinusoidal road input Disturbance	37
4.4	Simulation Results of Type A random road input at Four different vehicle speeds	40
4.5	Simulation Results of Type B random road input at four different vehicle speeds	50
4.6	Simulation Results of Type C random road input at four different vehicle speeds	58
4.7	Summery	66
CHAPTER FIVE		67
5	CONCLUSION AND RECOMMENDATION	67
5.1	Conclusion	67
5.2	Recommendation	67
5.3	Future work	68
Research fund Acknowledgment		69
APPENDIXES		72

LIST OF TABLES

Table 3.1 the parameters values	19
Table 3.2 Random Road type	25
Table 4.1: Comparison of peak to peak under two pumps	37
Table 4.2: Comparison of peak to peak under four pump	39
Table 4.3: peak to peak values of PSS using type A random input simulation.....	49
Table 4.4: peak to peak values of ASS using type A random input simulation	49
Table 4.5: peak to peak values of PSS using type B random road input simulation.....	57
Table 4.6: peak to peak values of ASS using type B random road input simulations.....	58
Table 4.7: peak to peak values of PSS using type C random road input simulations	65
Table 4.8: peak to peak values of ASS using type C random road input simulations.....	65

LIST OF FIGURE

Figure 3.1 Flow chart Methodology.	16
Figure 3.2 Active Quarter Car Suspension.	20
Figure 3.3 Two Pump Road profile input.	22
Figure 3.4 Four Pump Road Profile input.	23
Figure 3.5 A type Random Road input.	26
Figure 3.6 B type Random Road input.	26
Figure 3.7 C type Random Road input.	27
Figure 3.8 Step by step procedure to acquire parameters of NPID controller.	30
Figure 3.9 Popov Stability Criterion.	32
Figure 4.1 Simulation model for active quarter car suspension.	34
Figure 4.2 Two Pump Spring Acceleration with NPID controller.	35
Figure 4.3 Two Pump Suspension Deflection with NPID controller.	36
Figure 4.4 Two Pump Tire Deflection with and without NPID Controller.	36
Figure 4.5 Four Pump Spring Acceleration with and without NPID Controller.	37
Figure 4.6 Four Pump Suspension Deflection with and without NPID Controller.	38
Figure 4.7 Four Pump Tire Deflection with and without NPID Controller.	39
Figure 4.8 A Type Random Road Disturbance Spring Acceleration at 20km/hr.	40
Figure 4.9A type Random Road Disturbance Suspension Deflection at 20km/hr.	40
Figure 4.10 A type Random Road Disturbance Tire Deflection at 20m/hr.	41
Figure 4.11 A type Random Road Disturbance Spring Acceleration at 40km/hr.	42
Figure 4.12 A type Random Road Disturbance Spring Deflection at 40km/hr.	43
Figure 4.13 A type Random Road Disturbance Tire Deflection at 40km/hr.	43
Figure 4.14 A type Random Road Disturbance Spring Acceleration at 60km/hr.	44
Figure 4.15 A type Random Road Disturbance Suspension Deflection at 60km/hr.	45
Figure4.16 A type Random Road Disturbance Tire Deflection at 60km/hr.	46
Figure 4.17 A type Random Road Disturbance Spring Acceleration at 80km/hr.	47
Figure 4.18 A type Random Road Disturbance suspension deflection at 80km/hr.	47
Figure 4.19 A type Random Road Disturbance Tire Deflection at 80km/hr.	48

Figure 4.20 B type Random Road disturbance Spring Acceleration at 20km/hr.	50
Figure 4.21 B type Random Road Disturbance Suspension Deflection at 20km/hr.	50
Figure 4.22 B type Random Road Disturbance Tire Deflection at 20km/hr.	51
Figure 4.23 B type Random Road Disturbance Spring Acceleration at 40km/hr.	52
Figure 4.24 B type Random Road Disturbance Suspension Deflection at 40km/hr.	52
Figure 4.25 B type Random Road Disturbance Tire Deflection at 40km/hr.	53
Figure 4.26 B type Random Road Disturbance Spring Acceleration at 60km/hr.	53
Figure 4.27 B type Random Road Disturbance Suspension Deflection at 60km/hr.	54
Figure 4.28 B type Random Road Disturbance Tire Deflection at 60km/hr.	55
Figure 4.29 B type Random Road Disturbance Spring Acceleration at 80m/hr.	55
Figure 4.30 B type Random Road Disturbance Suspension Deflection at 80km/hr.	56
Figure 4.31 B type Random Road Disturbance Tire Deflection at 80km/hr.	57
Figure 4.32 C type Random Road Disturbance Spring Acceleration at 20km/hr.	58
Figure 4.33 C type Random Road Disturbance Suspension Deflection at 20km/hr.	59
Figure 4.34 C type Random Road Disturbance Tire Deflection at 20km/hr.	59
Figure 4.35 C type Random Road Disturbance Spring Acceleration at 40km/h.	60
Figure 4.36 C type Random Road Disturbance Suspension Deflection at 40km/hr.	60
Figure 4.37 C type Random Road Disturbance Tire Deflection at 40km/hr.	61
Figure 4.36 C type Random Road Disturbance Spring Acceleration at 60km/hr.	61
Figure 4.37 C type Random Road Disturbance Suspension Deflection at 60m/hr.	62
Figure 4.38 C type Random Road Disturbance Tire Deflection at 60km/hr.	63
Figure 4.39 C type Random Road Disturbance Spring Acceleration at 80m/hr.	63
Figure 4.40 C type Random Road Disturbance Suspension Deflection at 80km/hr.	64
Figure 4.41 C type Random Road Disturbance Tire Deflection at 80km/hr.	64

CHAPTER ONE

1 INTRODUCTION

Welcome to the realm of vehicle systems, where three dominant categories reign supreme: passive or inactive suspension systems, semi-active suspension systems, and active suspension systems. When it comes to passive suspension systems, the key to achieving a safe and comfortable ride lies in meticulous adjustments of the damping coefficient and the spring constant. However, this type of suspension system poses a challenge due to the delicate balance required between ride safety and comfort. For instance, minimizing vibrations of the vehicle body leads to enhanced ride comfort, while increasing the contact area between the car wheels and the road surface ensures ride safety. Unfortunately, an inactive suspension system struggles to optimize both aspects simultaneously, necessitating engineers to strike a compromise in order to design an effective suspension system. On the other hand, an active suspension system has the capability to harmonize ride safety and comfort concurrently, albeit at a higher cost and increased power consumption.

When faced with complex systems and increasing uncertain factors, the conventional linear PID controller falls short. Fortunately, the nonlinear PID controller rises to the occasion, reflecting the true nonlinear relationships between controlled variables and deviation signals, and overcoming some of the limitations of its linear counterpart (Greg Shinskey, 2017). In recent years, a plethora of methods have been employed to enhance the performance of the standard linear PID controller, resolving the contradictions between setting value trace and disturbance rejection, and improving both dynamic and static performance robustness and control performance.

The suspension system of a vehicle encompasses three crucial objectives: enhancing passenger comfort by reducing vertical body movements, minimizing tire deflection for improved handling performance, and adapting to load changes during various maneuvers. However, achieving the ideal balance between ride comforts and handling using a conventional passive suspension can be exceptionally challenging, even with state-of-the-art optimization techniques. To elucidate, while a soft spring and damper are necessary for

enhancing ride comfort, a stiffer suspension becomes essential during cornering or braking to ensure better control. Thankfully, advancements in computer technology, electronics, hydraulics, and control systems have given birth to a groundbreaking solution - the active suspension.

The suspension system serves as the driving force behind a vehicle's dynamic behavior, with its primary purpose being to mitigate the impacts of uneven road surfaces on passengers while maintaining wheel contact with the road to ensure stability and control. This study explores both passive and active suspension systems. Passive systems rely on traditional springs and dampers without feedback mechanisms to absorb road disturbances. On the other hand, active systems employ force actuators and closed-loop control, responding to input from the vehicle's vertical dynamics sensors to generate the necessary control force. Extensive research has examined the relationship between suspension systems, vehicle handling and stability, driver comfort, and safety. However, the complex mathematical relationships in nonlinear active suspension systems have led many researchers to approximate them as linear systems during controller design. Nevertheless, considering the nonlinear effects and uncertainties inherent in suspension systems, the use of nonlinear active suspension control laws becomes imperative.

In this thesis, I present a straightforward enhancement to the conventional PID controller that involves the integration of a non-linear gain in cascade with a linear fixed gain PID controller. This integration allows the controller to adapt its performance based on the characteristics of the closed-loop control system. The non-linear gain is activated when a significant deviation exists between the set point and the actual value of the controlled variable. In such instances, the gain substantially amplifies the error, leading to a substantial corrective action that efficiently drives the system output towards its desired target. As the error diminishes, the gain automatically reduces to prevent excessive overshoot in the response. This automatic adjustment of the gain provides the non-linear PID controller with a distinct advantage, offering a high initial gain for a rapid response and a low gain to mitigate large overshoots.

In the realm of control systems, the overarching objective is to attain rapid response, negligible steady-state error, and minimal overshoot, all while ensuring resilience against parameter uncertainties and disturbances. While incorporating an integral term in the

controller can aid in rejecting constant disturbances, it is known to inadvertently amplify the system's overshoot (Ang et al., 2005). To tackle this predicament, non-linear variable gain controller structures have been proposed to mitigate steady-state error resulting from disturbances(Hunnekens et al., 2014) .

The suspension system assumes a critical role in shaping the dynamic behavior of a vehicle. It serves to shield passengers from the harsh vibrations induced by uneven road surfaces and ensures optimal wheel contact with the road, thereby facilitating stability and control. This paper delves into an exploration of both passive and active suspension systems employed in vehicles. Passive systems rely on conventional springs and dampers, operating without any feedback mechanism to absorb road disturbances. On the other hand, active systems utilize force actuator elements within a closed-loop control framework, leveraging input from the vehicle's vertical dynamics sensors to generate the necessary control force. Extensive research efforts have been dedicated to investigating suspension systems, encompassing aspects such as vehicle handling, stability, driver comfort, and safety.

1.1 Statement of Problem

Suspension stands as a paramount concern, particularly within the automotive industry, where customers hold manufacturers accountable for any vibrations experienced by passengers. Vehicles encounter diverse external disturbances like bumps and potholes, which are transferred to passengers through the suspension system that physically separates the car's body from its wheels. To deliver a superior ride quality, a suspension system must effectively isolate the vehicle body from the wheels while also shielding the entire car from road disturbances. Moreover, passenger comfort can be achieved by minimizing the transmission of vertical forces arising from road disturbances. Hence, optimizing both the vertical displacement of the vehicle and suspension system travel, along with regulating the distribution of forces generated by external loads, becomes essential for attaining optimal performance. This thesis presents a comprehensive active quarter car suspension model used to tackle these challenges and proposes a nonlinear PID controller with an actuator for a viable solution.

1.2 Objectives of the study

1.2.1 General objective

The primary aim of this study is to design an optimal non-linear proportional-integral-derivative controller for an active quarter car suspension system.

1.2.2 Specific objective

- Model active suspension system for design controller.
- Computational analysis of hydraulic suspension with the MATLAB/SIMULINK package.
- Design different road profiles with selected vehicle speeds.
- Comparison of the analysis results to evaluate the performance based on ride comfort, road holding and suspension travel of the active car suspension with controller and without controller.

1.3 Scope of the Study

In this thesis, our focus lies in two main areas: deriving a mathematical model to capture the dynamics of a system and designing an optimal non-linear proportional-integral-derivative (NPID) controller for an active quarter car suspension system. The implementation of these objectives will be carried out using MATLAB/Simulink. It's important to note that this thesis will solely focus on the theoretical aspects of the research, and no hardware implementation will be undertaken.

1.4 Significant of project

The control of active quarter car suspension systems represents a pivotal research domain within the field of control systems. As the reliance on vehicles for daily transportation continues to grow, numerous countries are actively engaged in research endeavors aimed at exploring the advantages of controlling active quarter car suspension systems. These studies hold particular significance in terms of minimizing the transmission of vertical forces to passengers and optimizing tire-to-road contact to enhance handling and safety. The implementation of an optimal non-linear proportional-integral-derivative (NPID) controller for an active quarter car suspension offers a multitude of benefits.

- Firstly, it enhances passenger and vehicle safety while cornering and braking at different speeds.
- Secondly, it contributes to the advancement of automobile technology by improving the control algorithm of vehicle dynamics in the suspension system.
- Thirdly, it addresses customer concerns about vibrations being easily transferred to passengers and extends the life of vehicles.
- Finally, it serves as a starting point for researchers to explore other parameters of suspension, leading to further advancements in the field.

1.5 Outline of the Thesis

This thesis is organized into five chapters.

Chapter 1 The introduction provides a clear overview of the active suspension system in vehicles and highlights the observed issues. Furthermore, it briefly summarizes the overall tasks, literature reviews, scopes, and methods employed to achieve the main objective.

Chapter 2 The section begins by offering concise definitions, outlining the different types of suspension systems, and explaining their operational principles. It then proceeds to describe the derivation of nonlinear equations of motion for both the vehicle and the wheel. Following this, a suitable representation of the system's dynamic model is developed using state space representation, which serves as the foundation for the subsequent controller design.

Chapter 3 The design of an optimal nonlinear proportional integral derivative (NPID) controller for the suspension system of a vehicle is pursued. The primary objective of this control system is to minimize both suspension and tire deflection while maximizing road handling performance at an optimal value, accounting for varying road conditions.

Chapter 4 A nominal suspension system and an NPID-based suspension system of a vehicle were simulated in MATLAB. The performance of both systems was evaluated across different road scenarios and varying vehicle speeds. Finally,

Chapter 5 The work conducted and the results obtained are summarized, providing an overview of the accomplished tasks. Additionally, recommendations for future work are presented, identifying potential areas for further investigation and development.

CHAPTER TWO

2 LITERATURE REVIEW

The vehicle suspension system plays a critical role in both protecting the vehicle body from road disturbances and maintaining optimal road holding through continuous road-wheel contact. Achieving a delicate balance between ride comfort, handling quality, and road holding necessitates a trade-off within the suspension travel limits. Broadly categorized into passive, semi-active, and active systems, the dynamic behavior of passive suspension systems relies on fixed spring stiffness and damper coefficients, which may not provide sufficient energy absorption capability to withstand road disturbances, leading to instability. In contrast, semi-active suspension systems incorporate variable dampers or other dissipation components to enhance stability and performance.

(Sharkawy et al., 2015) conducted a study on implementing a PID controller for a quarter vehicle active suspension, resulting in significant improvement in control performance compared to passive suspension, notably, the researchers manually addressed parametric uncertainties, highlighting the importance of considering such factors in control systems. However, it is important to acknowledge that while linear control systems can enhance control performance, they have limitations in effectively addressing the complex nonlinearities and uncertainties inherent in the system.

(Ayele et al., 2020) proposed an enhanced optimal sliding mode (SM) controller for the nonlinear Active Vehicle Suspension System (AVSS) of a car, achieving exceptional nominal suspension performance and increased robustness. Through the utilization of linearized feed-forward and feedback techniques, they demonstrated the superior performance of the optimal sliding mode controller compared to the existing methods. The primary objectives of active suspension systems in vehicles encompass isolating the sprung mass from road disturbances and ensuring vehicle stability across diverse operating conditions.

The hydraulic actuator, powered by the Electro-Hydraulic Suspension System (EHSS), generates forces that strike a balance between ride comfort and road grip. Provided below is a

comprehensive list of nomenclatures along with their corresponding descriptions for the parameters of the active suspension system.

The passive suspension system's design falls short in catering to specific operating conditions, lacking the ability to adjust its parameters accordingly. Relying on fixed springs and dampers, its

(Meng et al., 2021) introduced an innovative control method utilizing a homogeneous domination approach to develop an active suspension homogeneous controller (ASHC). Meng's research indicated that the ASHC stabilizes the system within 2 seconds, while the sliding mode control (SMC) takes 2.5 seconds. However, when considering the dynamic equations of the hydraulic cylinder and servo valve, along with control system properties like the Bode diagram, it is recommended to employ a PID controller within the MATLAB SIMULINK environment. This is because the PID block offers a comprehensive characterization of the control system. Due to its straightforward structure and relative ease of tuning, either intuitively or through available tuning methods, PID control remains the preferred choice in industrial settings. Recent studies, such as ,(Shafieei, 2022) have concluded that active suspension systems controlled by PID controllers yield superior responses compared to passive systems.

2.1 Vehicle Dynamics Modeling

Passenger comfort has become a pivotal aspect in vehicle selection, given the increased amount of time individuals spend in their cars. Automobile manufacturers are actively striving to provide the utmost comfort by adapting their suspension systems to effectively handle load bumps and potholes. The presence of road roughness and bumps, which have a significant impact on ride comfort, remains a challenging factor for vehicle design engineers and drivers to control. Vehicle dynamics modeling involves creating a mathematical representation that accurately captures the behavior of a moving vehicle. This model takes into account various physical properties of the vehicle, such as mass, dimensions, and tire characteristics, as well as external forces including gravity, aerodynamic drag, and friction.

Vehicle dynamics modeling is a pivotal aspect in comprehending how a vehicle behaves across various dynamics modeling is a pivotal aspect in comprehending how a vehicle

behaves across various driving conditions, encompassing acceleration, braking, and turning. This understanding serves as the foundation for optimizing vehicle design to meet specific performance criteria, including stability, handling, and fuel efficiency. The approaches to vehicle dynamics modeling range from simple kinematic models, which solely consider motion, to complex multi-body models that meticulously simulate the behavior of each vehicle component. Vehicle dynamics modeling serves as an individual tool for engineers, designers, and researchers, enabling them to analyze and predict vehicle behavior in a safe and cost-effective manner, reducing the need for extensive testing on physical vehicles.

In recent literature, particular (Nagarkar et al., 2018), there has been a notable emphasis on preliminary research centered on the single-tire car suspension system. This specific vehicle model, commonly referred to as the quarter car model, has garnered considerable attention.

Moreover, the bicycle and half vehicle models represent advanced mathematical frameworks derived from the quarter car model. The bicycle car model takes into account two longitudinally aligned tires, while the half car model examines the behavior of two laterally aligned tires. Lastly, the full car model comprehensively investigates the suspension system of all tires, enabling a holistic comprehension of the vehicle's overall suspension dynamics.

2.1.1 Passive Suspension System

The suspension system of a vehicle, composed of springs and shock absorbers, serves the vital purpose of shielding both the vehicle chassis and its occupants from sudden vertical wheel assembly displacements during driving. Ensuring the comfort and safety of vehicle occupants, as well as the long-term durability of electronic and mechanical components, heavily relies on a well-tuned suspension system. While passive suspension systems possess fixed spring and damper characteristics tailored to specific performance objectives and intended applications, they lack the adaptability to adjust suspension stiffness and damping coefficients in response to varying road conditions or disturbance levels. To address this limitation, suspension control systems are engineered to dynamically alter the behavior of a vehicle's suspension system based on driving conditions and driver input, thereby enhancing ride comfort, handling, and overall stability.

2.1.2 Semi-active Suspension System

Embark on a journey into the realm of semi-active suspension systems, where unparalleled performance awaits. These cutting-edge systems surpass traditional passive suspensions by providing superior control over spring stiffness and damping coefficients. While adjusting spring stiffness has proven challenging, semi-active suspensions excel in seamlessly adapting damping coefficients to accommodate varying road conditions and disturbances that impact the vehicle's unsprung mass. Innovatively designed, semi-active suspensions streamline operations by eliminating the need for separate dynamic control components. Instead, they rely on feedback from suspension travel sensors to intelligently process road disturbances. This intelligent approach ensures optimal suspension states, precisely tailored to real-time road conditions. Prepare to indulge in unparalleled comfort as both drivers and passengers revel in the sublime smoothness delivered by semi-active suspensions, effortlessly surpassing their passive counterparts.

Moreover, the inclusion of controllable dampers significantly enhances vehicle handling, elevating the driving experience to new heights of safety and enjoyment. Experience the difference as you navigate the roads with utmost confidence and grace, courtesy of semi-active suspensions.

2.1.3 Active Suspension System

Experience the cutting-edge innovation of active suspension system, a modern evolution in suspension technology. Equipped with a dedicated dynamic control component, active suspensions expertly counteract road disturbances, ensuring a smooth and comfortable ride.

Requiring a constant power source, transmission mechanism, and a sophisticated sensory network with microcontroller integration, active suspension systems boast the ability to adapt damping force in response to varying road conditions. This advanced multi-mode control enhances vehicle handling performance and stability, surpassing the capabilities of both passive and semi-active suspension systems. Additionally, active suspensions elevate cornering abilities by reacting to inertia and counteracting spring deformation during turns, providing drivers with superior control and confidence on the road.

Explore the diverse world of suspension control systems, featuring active, semi active, and adaptive suspension technologies. Active suspension systems employ hydraulic or electrical actuators to dynamically fine-tune damping and stiffness, while semi-active systems utilize adjustable dampers governed by an electronic control unit. Adaptive suspensions, on the other hand, rely on sensors to monitor driving conditions, adjusting in real-time for optimal comfort and handling. These advanced suspension control systems elevate vehicle performance in numerous ways, including reducing body roll during cornering, enhancing traction during accelerating and braking, and mitigating the impact of road imperfections. Additionally, they contribute to improved stability at high speeds and alleviate driver fatigue and discomfort on extended journeys. Experience the growing prevalence of suspension control systems in today's automotive landscape, prominently featured in high-performance sports cars and luxury vehicles. These systems also enhance safety and comfort in commercial vehicles, such as trucks and buses, benefiting both passengers and cargo. Suspension systems span a range of categories, including passive, semi-active, and fully active. Early studies (Azizi & Mobki, 2021) on passive suspension systems focused on energy-storing elements and dampers with fixed characteristics. However, their performance is limited and can only be altered by modifying damper and spring properties, with no controller for energy input or dissipation. A heavily damped system offers superior road handling at the expense of ride quality, while a lightly damped system delivers a comfortable ride but compromises road handling. Semi-active suspension systems, on the other hand, provide controlled damping with fixed spring characteristics. These innovative systems are expertly designed to manage energy dissipation in a controlled manner.

2.2 Hydraulic active suspension system

Experience the dynamic performance of hydraulic active suspension systems, which employ hydraulic actuators to seamlessly adjust damping and stiffness in real-time. These systems feature hydraulic actuators connected to each wheel's suspension, governed by a hydraulic pump and an electronic control unit (ECU). The ECU receives input from sensors that monitor driving conditions and driver input. Upon detecting changes in driving conditions, such as

sharp turns or sudden terrain shifts, the ECU signals the hydraulic pump to modify the pressure within the actuators, altering the suspension system's damping and stiffness.

This adaptive capability ensures optimal ride comfort and handling, adjusting effortlessly to ever-changing driving conditions. Embrace the exceptional control offered by hydraulic active suspension systems, renowned for their rapid responsiveness to ever-changing driving conditions. These systems enable real-time suspension adjustments, delivering optimal performance and enhancing handling, stability, and ride comfort especially in high-performance vehicles. Despite their advantages, hydraulic active suspension systems can be intricate and costly to design, produce, and maintain. Consequently, they are predominantly featured in high-end luxury vehicles and sports cars, rather than in mass-market automobiles.

2.3 Review of Related Literatures

In today's automotive market, passengers and car buyers seek luxurious vehicles that offer support, safety, ride comfort, road holding, and suspension deflection. Over the years, researchers have focused on ensuring suspension system stability and enhancing performance aspects such as ride comfort (directly related to passenger-experienced acceleration), suspension deflection (the displacement between sprung and unsprung masses), and road handling (associated with tire contact forces and road surfaces).

Youness and Lobusov developed a 7 DOF vehicle model using PID and LQR controllers (Rizvi et al., 2018). Their findings suggest that the LQR controller offers greater flexibility in selecting direct control parameters, while PID still delivers satisfactory results for controlling suspension travel. In networked systems, LQR outperforms PID at lower network speeds, although the controllers lack robustness. P. Gandhi et al. examined a 4 DOF mathematical model of a half-vehicle using PID, LQR, Fuzzy, and ANFIS controllers (Gandhi et al., 2017). The performance of these controllers was tested with random road input and compared to conventional PSS.

S.M.H. Rizvi and colleagues delved into the world of mathematical modeling to create a full vehicle model with a design H_{∞} controller (Taskin et al., 2017). Their goal was to minimize the impact of road disturbances on both the vehicle and its passengers. After testing the performance of their ASS, they were thrilled to discover that it led to even better results.

Meanwhile, V. Pontevedra tackled a similar challenge by developing a mathematical model of a quarter vehicle model and implementing PID and LQR control (Azizi & Mobki, 2021). They put the model through its paces with a Class C type random road input at 80Km/hr, and even went so far as to model a GA based optimization function as a multi-objective problem. The outcome? Optimized parameters outperformed both classical parameters and PSS. While the PID controller effectively reduced RMS acceleration and VDV, it's worth noting that the controllers used were not particularly robust.

S. Rajala and colleagues took on the challenge of studying a mathematical model of a quarter vehicle model, and they did so by designing an H_{∞} control (Youness & Lobusov, 2019). Through simulations and real test track data, they evaluated the controller's performance and found that it offered significant advantages over its predecessor. The suspension performance was notably improved, though it's worth noting that perturbation and unmodeled dynamics were not taken into consideration.

Meanwhile, H.P. Wang and team tackled a similar challenge by developing a mathematical model of a quarter vehicle model and implementing MFOSMC (H. P. Wang et al., 2018). They even went so far as to compare their Co-Simulation Platform with PID, TDEC, and classic PID controllers. The results were encouraging, as the MFOSMC achieved a reasonable control performance that met the system requirements. However, it's important to note that perturbation and unmodeled dynamics were not taken into account.

To take advantage of this approach, an active suspension system was implemented to enhance the performance of the suspension system. Each wheel is equipped with a hydraulic actuator, whose operation is dependent on the opening and closing of servo valves. The controller's current signal controls the opening and closing of these gates, which in turn results in the hydraulic actuator exerting force on the spring-loaded and un-sprung masses. This force is harnessed to dampen the vehicle's vibrations, resulting in a substantially smoother ride, as reported by Nguyen(H. P. Wang et al., 2018) .

In recent years, there have been numerous advancements in control algorithms for active suspension systems. For instance, explored the use of PID (Proportional-Derivative-Integral) control techniques in their work.

Kararsiz and colleagues, on the other hand, opted for the HILS method in their studies (Shafiei, 2022). Their research focused on semi-active suspension systems, with the road disturbance represented by the sum of sinusoidal waves with unknown coefficients.

(Omar et al., 2018) developed a nonlinear 4 DOF half vehicle model featuring an active suspension system, which was governed by a PID controller. Although the model ignored nonlinearities in the hydraulic actuator due to their minimal impact, it was constructed using Matlab/Simulink.

The major research gap identified from the different literatures is that many researchers considered vehicle suspension as a linear system for the matter of simplicity of mathematical modelling. But, in practical terms vehicle suspension is a nonlinear system because it consists of flexible suspension tires and other components which have nonlinear properties, such as nonlinear spring and damper. Also, it is found that most of the vehicles now a days have a passive suspension system, which is simulated and designed without the consideration of nonlinearities on the spring and damper. That design affects the ride comfort performance of the vehicle, especially when the spring and damper are subjected to large deflection and velocity respectively due to different off road conditions. Conventional linear PID controller is not effective when the system is more complex and uncertain factors of object increase. However, the nonlinear PID controller, which reflects the non-linear relations of the controlled variables and the deviation signal veritably, can overcome the disadvantages of the linear PID controller to some extent. In recent years, many methods have been adopted to improve the routine linear PID controller against the contradictions between setting value trace and disturbance rejection, dynamic and static performance, robust and control Performance.

CHAPTER THREE

3 METHODOLOGY

In this chapter, we delve into the key components of the study, including the material and methods used, vehicle specifications, suspension models, passive and NPID controller designs aimed at Minimizing errors, and simulations. To analyze the vehicle dynamics, we utilized the powerful MATLAB/SIMULINK software.

3.1 Materials

The tools used for this thesis work are both powerful and versatile. For instance, we employed MATLAB software for developing the vehicle model and simulating various parts of a quarter-car suspension system.

To evaluate the performance of the suspension system, we relied on the MATLAB/Simulink software package, which offered a range of powerful tools for analysis. MATLAB itself is a matrix-based system software that is ideal for writing programs to solve complex mathematical, scientific, and engineering calculations. In this work, we utilized MATLAB extensively for analyzing and designing control systems, including generating transfer functions and state-space representations, determining system stability and observability, and analyzing frequency responses to different input signals. Additionally, we relied on MATLAB to solve algebraic Raccati equations and other complex mathematical problems.

3.2 Methodology

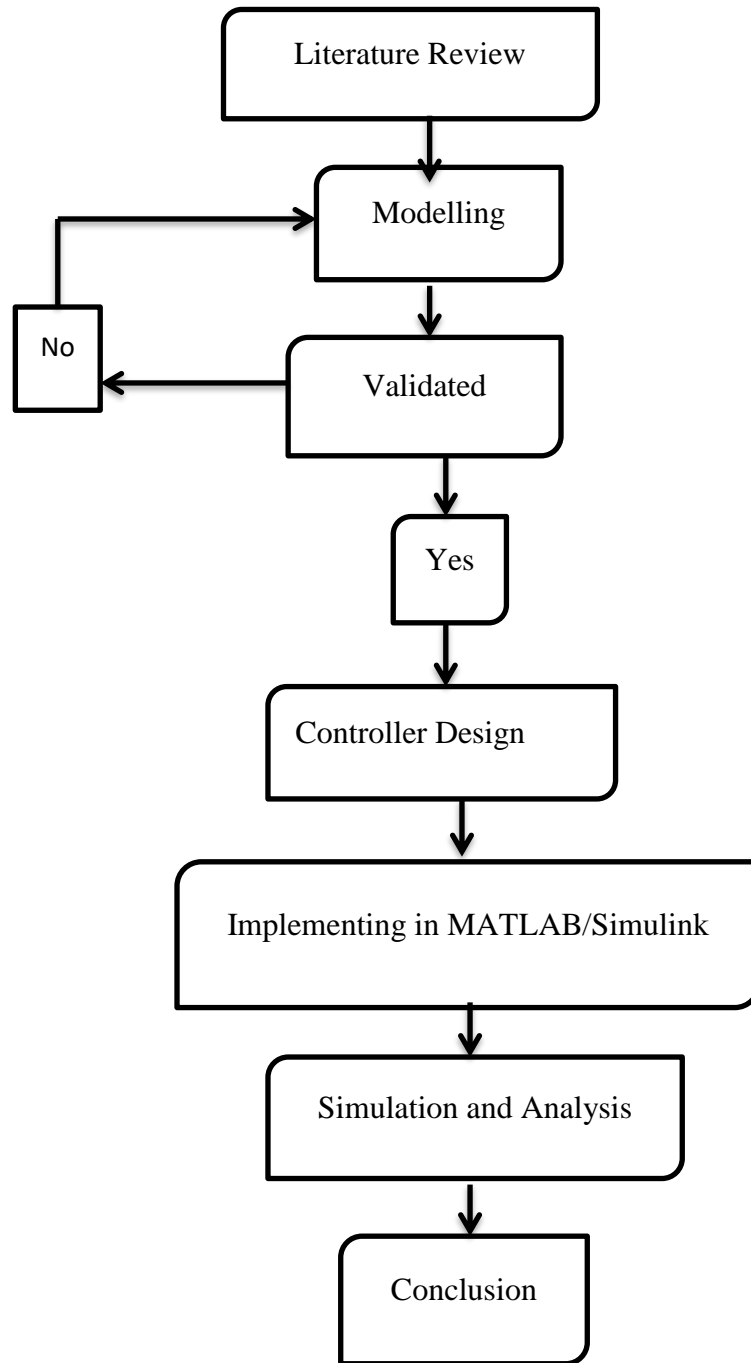


Figure 3.1 Flow chart Methodology.

To achieve the objectives of this thesis, we first conducted a comprehensive literature survey to Review previous research on vehicle vibration modeling and controller design for improving ride quality and road handling. Then, we derived the mathematical models for both the active suspension system (ASS) and passive suspension system (PSS) for comparison purposes. Developing an hydraulic suspension model with a controller for passenger car application requires a robust mathematical model as a foundation, and an extensive study was conducted to select the most suitable model for an active suspension system. In this study, I opted for the quarter-car model, which offers a detailed and accurate understanding of vehicle dynamics. External input disturbances in the form of road bumps were modeled to simulate real-world conditions.

Next, I validated the derived mathematical model through literature work and proceeded to design NPID controllers for the quarter-car model suspension system, with the goal of improving performance compared to other control methods used in prior studies. Then implemented the mathematical model and controller in the MATLAB/Simulink software for simulation purposes. Finally, I analyzed the simulation results of the ASS by comparing them to the PSS, in order to assess the efficacy of our approach. The working methodology applied during this thesis is listed below, in sequential steps for clarity.

3.3 Actuator Modeling

3.3.1 Hydraulic active suspension system

The control system employed in developing an active suspension system. This system utilizes several hydraulic components, including a pressurized hydraulic fluid source, a pressure relief valve for regulating the hydraulic fluid pressure, a direction control valve, and a hydraulic cylinder (active actuator) that converts hydraulic pressure into force, enabling transmission between the sprung and unsprung mass. Experience the power of advanced hydraulic servomechanisms, designed to seamlessly control cutting-edge hydraulically actuated suspensions. Driven by a high-pressure radial piston hydraulic pump, these systems deliver exceptional performance and reliability. State-of-the-art sensors continuously monitor body movement and vehicle ride level, transmitting real-time data to the onboard computer for optimal control.

As the computer processes this valuable information, it expertly operates the hydraulic servos strategically positioned beside each wheel. These servo-regulated suspensions generate counter forces, effectively combating body lean, dive, and squat during dynamic driving maneuvers.

Hydraulic actuators stand out as a top choice, thanks to their impressive power-to-weight ratio, cost-effectiveness, and ability to generate force over extended periods without overheating.

A hydraulic pump, often enhanced with accumulators to minimize pressure fluctuations and provide additional fluid during peak demands, supplies the necessary hydraulic pressure. The piston's position within the hydraulic cylinder can be adjusted by modulating oil flow in and out of the cylinder chambers, connected to the spool valve via cylindrical ports. This precise modulation is expertly managed by the spool valve, ensuring a smooth and responsive driving experience. Hydraulic actuators are highly regarded for their exceptional power density, pinpoint control, and resilience in challenging environments. Frequently favored over alternative actuators like electric or pneumatic options, they excel in applications demanding substantial force and unparalleled precision.

3.4 Car suspension

Active suspension systems boast the remarkable ability to continuously reduce acceleration of sprung mass and minimize suspension deflection. This enhancement leads to improved tire grip on the road surface, significantly boosting braking, traction control, and overall vehicle maneuverability. In today's fiercely competitive automotive landscape, the race is on to develop cutting-edge models with superior performance capabilities.

Advanced suspension systems are a key performance requirement, expertly mitigating road disturbances to ensure passenger comfort while delivering a smooth, controlled driving experience. Although the primary goal of suspension systems is to provide a comfortable ride and maintain vehicle control over rough terrain or during sudden stops, increased ride comfort necessitates a larger suspension stroke and reduced damping in wheel hop mode.

3.5 Vehicle Suspension Model and Measurements

Vehicle suspension systems can be represented through various models, such as a quarter car with 2 degrees of freedom (DOF), a half-car with 4 DOF, or a full car with 7 DOF systems. In this study, I've chosen the quarter-car 2DOF model for analysis, as it strikes the perfect balance between providing valuable insights into suspension performance and maintaining optimal complexity. Figure 3.2 illustrates the quarter-car active suspension system model, complete with the essential mathematical model equations. As depicted in the figure, the active system features a control unit situated between the sprung mass and unsprung mass for the suspension systems.

Table 3.1 the parameters values

Coefficient	Definition	Value	Unit
M_{us}	Unsprung mass	41.5	Kg
M_s	Sprung mass	241.5	Kg
K_s	Spring stiffness	6.0×10^3	N/m
K_t	Tire stiffness	1.4×10^4	N/m
C_s	Spring damping	300	N.s/m
C_t	Tire damping	1500	N.s/m
Z_{us}	Unsprung mass displacement		M
Z_s	Sprung mass displacement		M
Z_r	Road profile		M
A_p	Actuator piston area	1.1×10^{-3}	M^2
V_t	The total volume of the chamber	1.1×10^{-4}	M^3
C_{tp}	Total leakage coefficient	1.0×10^{-11}	M^5/N
β_e	Effective bulk modulus	8.0×10^8	N/m^2
P_s	Supply pressure	2.1×10^7	N/m^2
T	Servo valve time constant	4.5×10^{-3}	S

K_{VA}	Voltage to ampere constant	1.00×10^{-3}	A/V
K_{MV}	Meter to voltage conversion gain	100	V/M

Table 3.1 shows the quarter car model's data and its actuator in the suspension system(X. Wang, 2017).

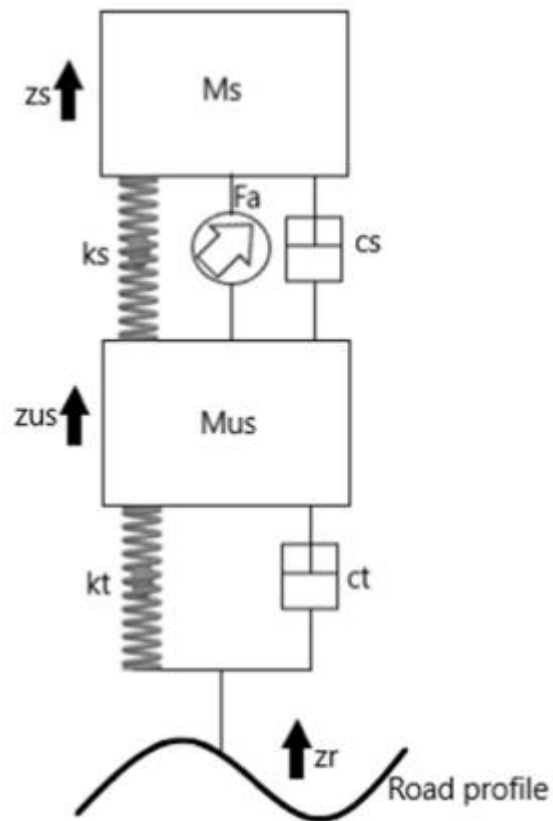


Figure 3.2 Active Quarter Car Suspension.

The active suspension system expertly applies a precise amount of force to both the wheel (unsprung mass) and body (spring mass), enabling the comprehensive control system to achieve the desired input seamlessly(et al., 2018).

The equation of motion based on Newton's law are given as

$$M_s \ddot{z}_s + k_s (z_s - z_{us}) + c_s (\dot{z}_s - \dot{z}_{us}) - F_a = 0 \quad (3.1)$$

$$M_{us} \ddot{z}_{us} + c_t (\dot{z}_{us} - \dot{z}_r) + k_s (z_{us} - z_s) + c_s (\ddot{z}_{us} - \ddot{z}_s) + k_t (z_{us} - z_r) + F_a = 0 \quad (3.2)$$

Where Z_r is road profile and F_a is actuator force ($F_a = A_p P_l$) Further by assuming $z_s = x_1$, $z_{us} = x_3$, $Z_r = x_r$, $P_l = x_5$ and $x_v = x_6$

Can be rewritten in the form of first-order differential equations as below

$$\dot{x}_1 = x_2 \quad (3.3)$$

$$\dot{x}_2 = -\frac{k_s}{m_s} x_1 - \frac{C_s}{m_s} x_2 + \frac{k_s}{m_s} x_3 + \frac{C_s}{m_s} x_4 + \frac{A_p}{m_s} x_5 \quad (3.4)$$

$$\dot{x}_3 = x_4 \quad (3.5)$$

$$\dot{x}_4 = +\frac{k_s}{m_{us}} x_1 + \frac{C_s}{m_{us}} x_2 - \frac{k_s + k_t}{m_{us}} x_3 - \frac{C_s + C_t}{m_{us}} x_4 - \frac{A_p}{m_{us}} x_5 + \frac{k_t}{m_{us}} x_r \quad (3.6)$$

$$\dot{x}_5 = -\alpha(x_2 - x_4) - \beta x_5 + \gamma x_6 (\sqrt{P_s} - x_5 \operatorname{sgn}(x_6)) \quad (3.7)$$

$$\dot{x}_6 = \frac{1}{\tau} \left(-x_6 + \frac{k_{VA}}{\tau} u \right) \quad (3.8)$$

Where $\alpha = 4A\beta_e / V_t$, $\beta = 4C_{tp} / V_t$, and $\gamma = 4C_d \beta_e w / (V_t \sqrt{\rho})$

$$A = \begin{bmatrix} -36.42 & 0.2797 & -342.9 & 0 & 2.253 \times 10^{-15} \\ 0.04807 & -0.04807 & 0.9613 & 0 & 3.855 \times 10^{-16} \\ 1 & 0 & 0 & 0 & 0 \\ 0.004807 & -0.004807 & -0.9613 & -222.2 & -3.855 \times 10^{-17} \\ 0.0011 & -0.0011 & 0 & 7.644 & -2.188 \times 10^{-20} \end{bmatrix}$$

$$B = \begin{bmatrix} 0 \\ 0 \\ 0 \\ 0.001 \\ 0 \end{bmatrix}$$

$$C = [0.04807 \quad -0.04807 \quad 0.9613 \quad 0 \quad 3.855 \times 10^{-16}]$$

$$D = 0$$

3.5 Road Profile

3.5.1 Two bump sinusoidal road profile

In this design, we utilize a two-bumpy sinusoidal road profile, where 'a' represents the bump amplitude, set at a value of 0.05m. Characterized by a 2Hz frequency, the sinusoidal bump is described by the equation provided above, serving as an input disturbance for the quarter car model. Figure 3.3 showcases the simulation of this input road disturbance for the quarter car, effectively illustrating the disturbance input.

$$\begin{cases} \frac{0.05}{2}(1 - \cos(2\pi * u / (0.5))) & \text{for } 0.5 \leq t \leq 0.75 \\ \frac{0.075}{2}(1 - \cos(2\pi * u / (1))) & \text{for } 6 \leq t \leq 6.5 \\ 0 & \text{otherwise} \end{cases} \quad (9)$$

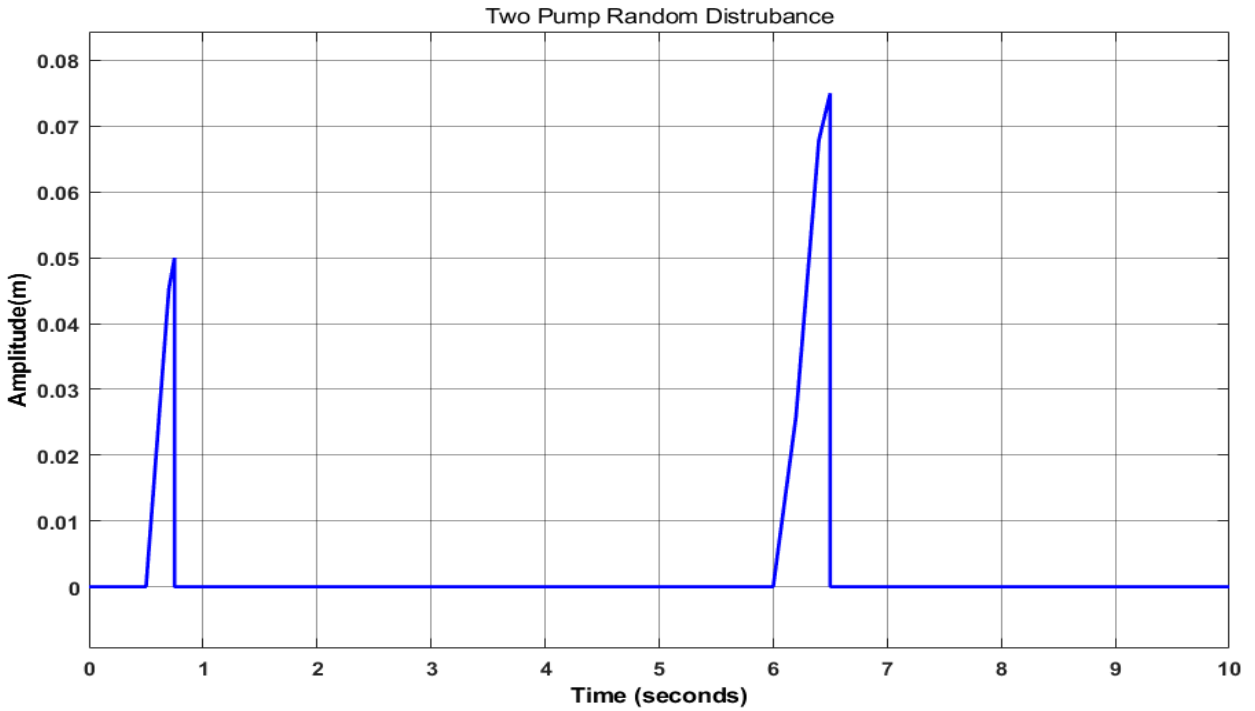


Figure 3.3 Two Pump Road profile input.

3.5.2 Four bump sinusoidal road profile

Four bumpy sinusoidal road profile is designed here, where a denotes the bump amplitude and its value $0.05m$ is taken. The sinusoidal bump with $2Hz$ frequency has been characterized by

$$\begin{cases} \frac{0.05}{2}(1 - \cos(2\pi * u / (0.5))) & \text{for } 0.5 \leq t \leq 0.75 \\ \frac{0.075}{2}(1 - \cos(2\pi * u / (1))) & \text{for } 3 \leq t \leq 3.25 \\ \frac{0.1}{2}(1 - \cos(2\pi * u / (1.25))) & \text{for } 5 \leq t \leq 5.25 \\ \frac{0.125}{2}(1 - \cos(2\pi * u / (1.5))) & \text{for } 6 \leq t \leq 6.25 \\ 0 & \text{otherwise} \end{cases} \quad (10)$$

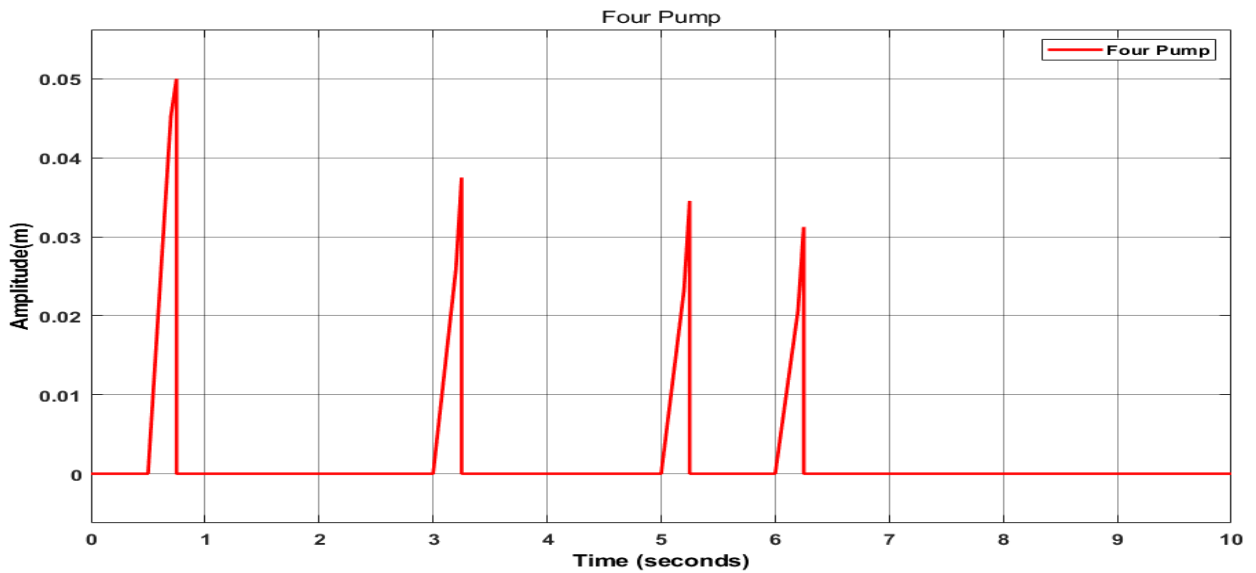


Figure 3.4 Four Pump Road Profile input.

3.5.3 Random Road profile

Road input as ISO 8608 random road profile

Imagine a world where roads and highways are smooth like silk, providing a comfortable ride for all. ISO, the International Organization for Standardization, is at the forefront of this vision, bringing together national standards bodies from around the globe in a worldwide federation. One of their key contributions is ISO 8608, a standard that lays out a uniform method for reporting and analyzing vertical surface profile data from various circumstances, including off-road terrains. By utilizing the standard methods of power spectral density (PSD), the quality of road surfaces can be evaluated with precision and accuracy, paving the way for safer and more comfortable journeys.

Random type road profiles offer the most accurate representation of real-world road inputs. In this research, we utilize classifications of road roughness based on ISO standards, as shown in Table 3.1. designed random type A (smooth) ,type B ,and C (rough) road inputs at four distinct vehicle operating speeds (20km/hr, 40km/hr, 60km/hr and 80km/hr) to demonstrate the effects of road roughness and vehicle speeds, while also aiming to enhance ride quality and road handling, as per the International Standard Organization.

ISO=TC108=SC2N67 as shown in Table 3.1, the road displacements are divided into several classes according to the degree of road roughness. When the speed is fixed, the speed of time domain power spectrum is white noise signal, the spectral density constant $4\pi^2 n_0^2 G(n_0) v$. The formula is described as

$$\dot{x}_r = 2\pi f_0 x_r + 2\pi n_0 \sqrt{G(n_0) v} w(t) \quad (3.11)$$

In the formula, $f_0 = 0.2$ is the cut off frequency and $2\pi n_0 \sqrt{G(n_0) v}$; is white noise. The power spectral values for type A, type B and type C random road type are $G(n_0) = 16 \times 10^{-6} m^3$; $n_0 = 0.1 m^{-1}$ and $G(n_0) = 256 \times 10^{-6} m^3$; $n_0 = 0.1 m^{-1}$

Respectively. The simulation is performed at 20km/hr; 40km/hr, 60km/hr and 80km/hr for both random road profiles. The simulations of class A, class B and class C type random

road profiles are given in figure 3.5, 3.6 and figure 3.7. The result shows that a vehicle experiences high disturbances (high RMS value) when the vehicle runs at high speed than low speed as well as it runs at rough surface than smooth surface road profile.

Table 3.2 Random Road type

Road type	$G_q(n_0) / 10^{-6} m^3 (n_0 = 0.1 m^{-1})$	$\sigma_q(n_0) / 10^{-3} (0.011 m^{-1} < n < 2.83 m^{-1})$
A	16	3.81
B	64	7.61
C	256	15.23
D	1024	30.45
E	4096	60.9
F	16384	127.6
G	65536	243.6
H	262144	487.22

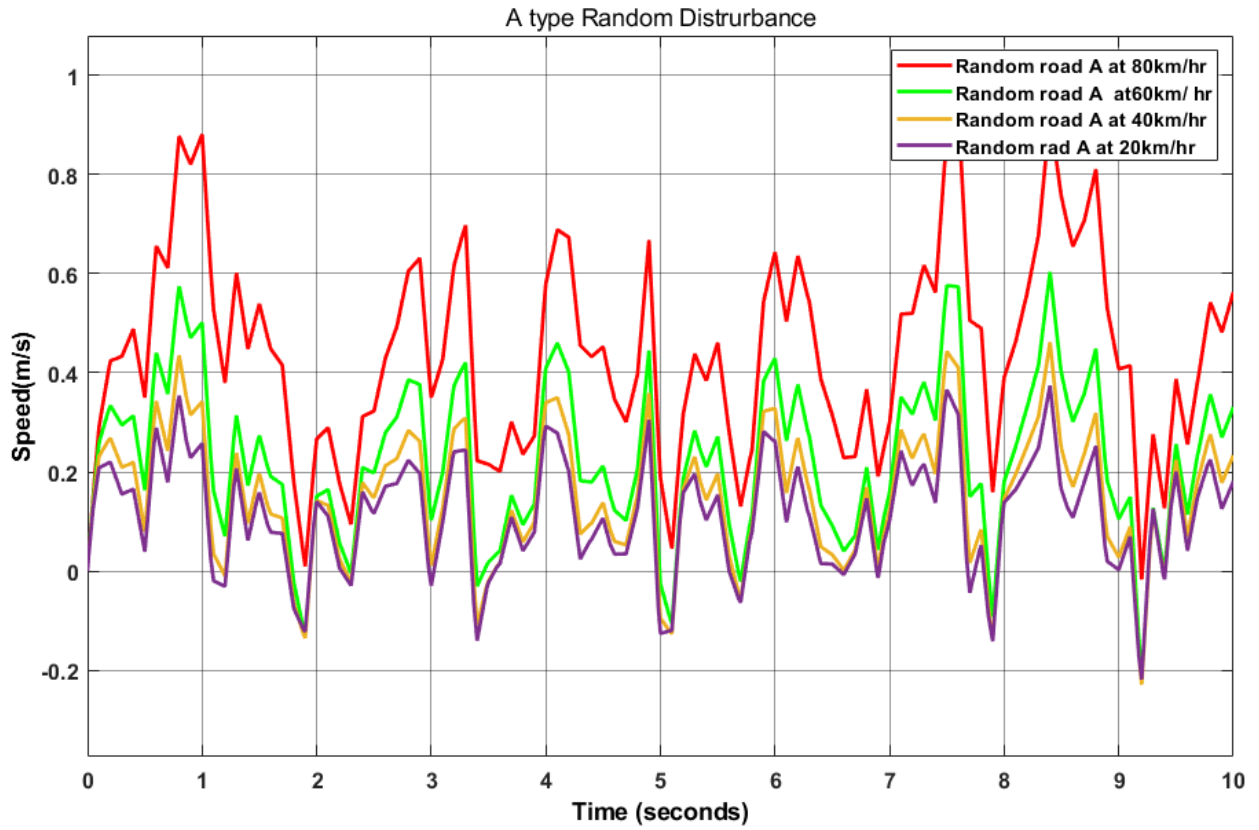


Figure 3.5 A type Random Road input.

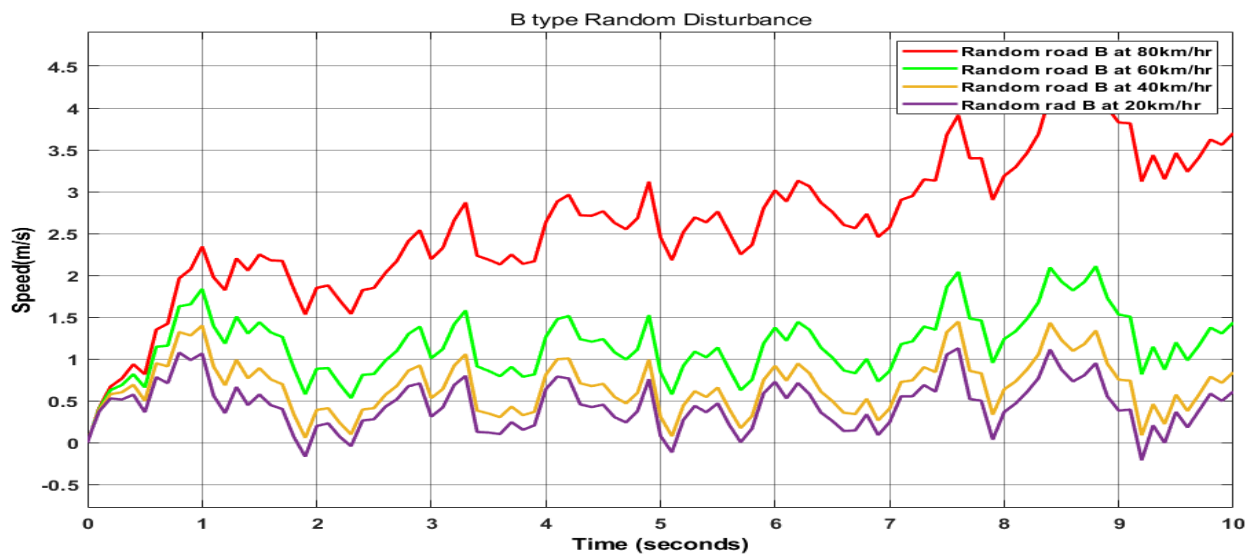


Figure 3.6 B type Random Road input.

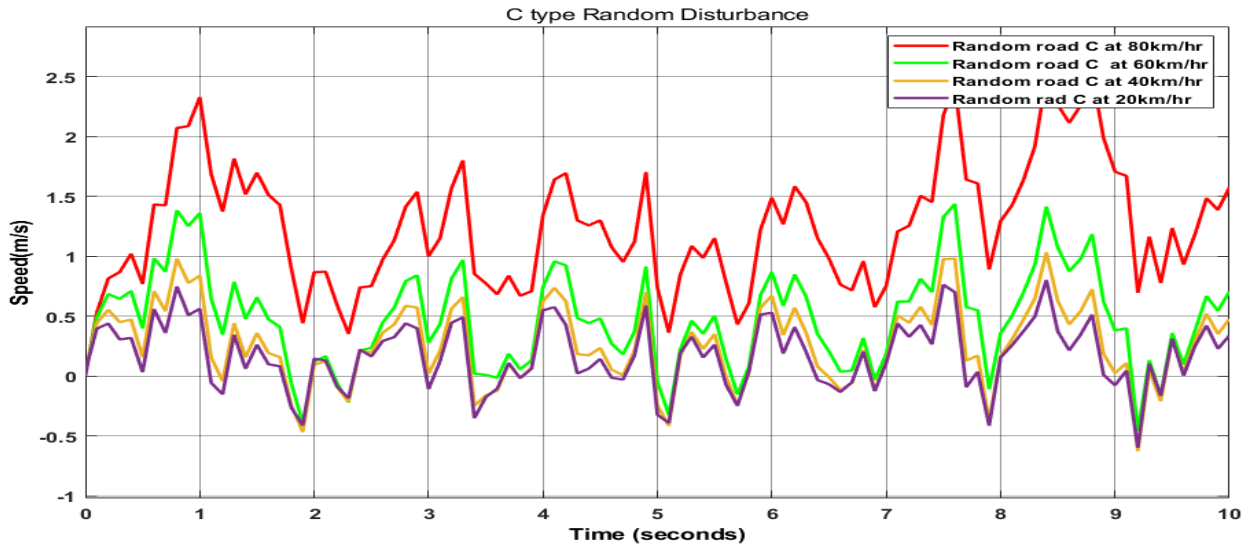


Figure 3.7 C type Random Road input.

To put the vehicle control system to the test, a simulation was conducted using a random road input. Figures 3.5, 3.6 and 3.7 display the A, B and C type road surfaces that were simulated on the vehicle, respectively. Interestingly, as the vehicle speed increased, the road profile changed and the spectral density increased accordingly, as evidenced by the simulated graph. To tackle this challenge, a new model was developed with a cutting-edge controller that enables the suspension system to perform flawlessly even at high speeds and on rough surfaces. With this innovation, drivers can enjoy a smoother, more stable ride without any compromise on performance.

3.6 Controller system design

3.6.1 Non Linear PID Controller

Let me take a stab at rewriting the sentence in a more appealing way: As illustrated in Fig. 3.8, e_{max} and K_e exhibit a linear proportional relationship. The rationale behind this correlation lies in the fact that a larger e_{max} value leads to a more aggressive behavior from the NPID controller, thanks to the bigger K_e value. This is because higher error requires higher gain to correct the system, which consequently has a significant impact on the system. Conversely,

opting for a smaller e_{\max} value results in a slow reaction from the NPID controller, owing to the smaller K_e value.

Nonlinear control systems take center stage when nonlinearity significantly influences either the controlled process (plant) or the controller itself. These systems are prevalent in a wide array of engineering and natural systems, encompassing mechanical and biological systems, aerospace and automotive control, industrial process control, and more. A control system featuring at least one nonlinear element is referred to as a nonlinear control system. This nonlinear factor represents the static characteristic between input and output that defies a linear relationship. The realm of nonlinear control systems encompasses all mathematical relationships, excluding linear ones.

The nonlinear PID (NPID) controller is a cutting-edge innovation that employs a sector-bounded nonlinear gain, $K(e)$, which is integrated in series (cascade) with a traditional PID controller. The parameters of the traditional PID controller were acquired based on prior research (Abdullah et al., 2013), which was grounded in the desired gain and phase margin.

Nonlineargain,

$$K(e) = \frac{\exp(ae) + \exp(-ae)}{2} \quad (3.12)$$

Error

$$e = \begin{cases} e & \text{if } |e| \leq e_{\max} \\ e_{\max} * \text{sign}(e) & \text{else } |e| > e_{\max} \end{cases} \quad (3.13)$$

$$K(e_{\max}) = \frac{1}{|G(j\omega)|} \quad (3.14)$$

Scaled Error

$$fe = ke \times e(t) \quad (3.15)$$

General transfer function of NPID controller

$$G_{NPID}(s) = [K_p * f_e] + \left[\frac{K_i}{s} * f_e \right] + [K_d s * f_e] \quad (3.16)$$

The self-tuned gain adjustment, $K(e)$, behaves as a nonlinear function of the error, $e(t)$, and is bounded within the sector $0 \leq K(e) \leq K(e_{max})$ as described in equations (12) and (13). These equations define the range of available choices for the nonlinear gain, $K(e)$. The output generated by this nonlinear function is known as the scaled error, f_e , and its equation is presented in (15). Alternatively, the overall equation of the NPID controller can be viewed as shown in (16).

3.6.2 Guidelines to obtain parameters of NPID controller

To design the NPID controller, we first needed to determine the parameters of the PID controller. Once these were established, we moved on to determining the rate variation of the nonlinear gain, α , and ultimately determining the range of variation error, e_{max} . This stepwise approach allowed us to develop a robust and effective NPID controller for the system.

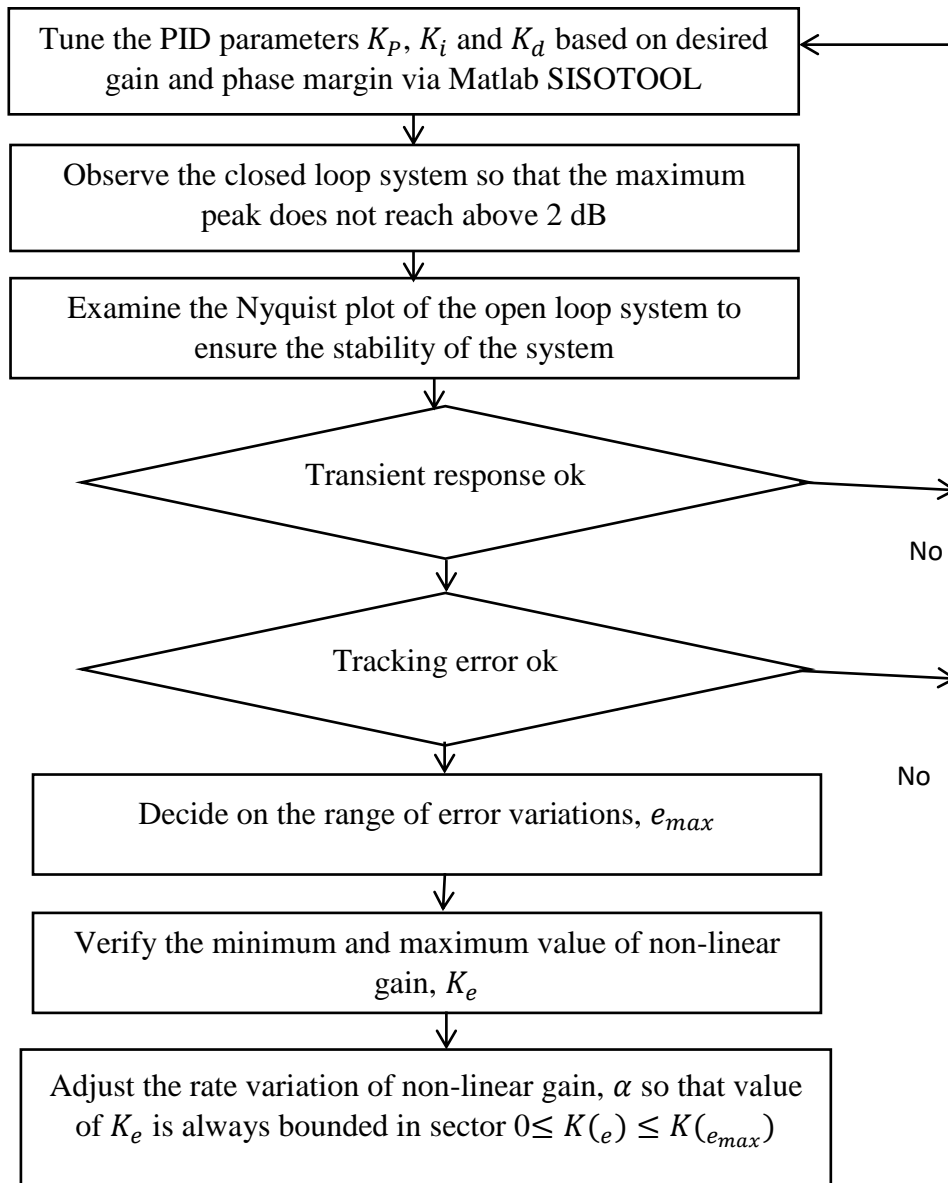


Figure 3.8 Step by step procedure to acquire parameters of NPID controller

3.7 Stability Test

The values of α and e_{max} , which respectively represent the rate of variation of nonlinear gain and the range of error variation, are crucial in determining the highest allowable value of nonlinear gain, $K(e)$, for ensuring stability. While the Nyquist plot suffices for fixed values of a PID controller, it becomes unreliable for an NPID controller, where the scaled error, f_e , keeps changing. In such cases, the Popov or Lyapunov stability criterion proves handy in determining stability. Employing the Popov stability criterion method, the authors were able

to verify stability as shown in Fig. 8. Further, the criterion was utilized to decide the value of $K(e)$, with detailed procedures described in previous research (I. et al., 2018). By manipulating the Matlab software, the Popov plot of $G(j\omega)$ was shown to intercept the negative real axis at the point $(-0.2, j0)$ as depicted in Fig. 3.9 Accordingly, the maximum value of the nonlinear gain, $K(e_{max})$, was determined using equation (3), leading to an allowable range of $K(e)$ between 0 and 3.

In this thesis, we explore the relationship between the nonlinear gain (represented by α) and error variation (represented by e_{max}) in the context of NPID controllers. To ensure stability, we select values of 1 for α and 3 for e_{max} based on the allowable range of nonlinear gain, $K(e)$. While the Nyquist plot is typically used for stability testing with fixed PID controllers, it is not applicable for NPID controllers where the value of scaled error, f_e , is constantly changing. Instead, we employ the Popov stability criterion, as shown in Figure 3.9 to determine the stability and maximum allowable value of $K(e)$ (which we calculate to be between 0 and 3). By analyzing the Popov plot of $G(j\omega)$, we find that the system is stable as P lies to the right of the intercept line at the negative real axis, indicating that our theoretical model is sound.

NPID control can be applied in two contexts: the first deals with nonlinear systems, where it is used to absorb nonlinearity; the second deals with linear systems, where it enhances performance beyond what is achievable with a linear PID control, e.g., by reducing overshoot, shortening rise time for step or rapid command inputs, and improving tracking accuracy while compensating for nonlinearity and disturbances. NPID controllers have the advantage of high initial gain, enabling a fast dynamic response, followed by low gain to maintain stability. The proposed controller provides several benefits, including easy implementation and mitigation of integrator windup by scaling down large input errors. Future studies should address stability issues under process parameter uncertainties using tools such as Popov and Circle criteria. Seraji has derived simple expressions for this purpose.

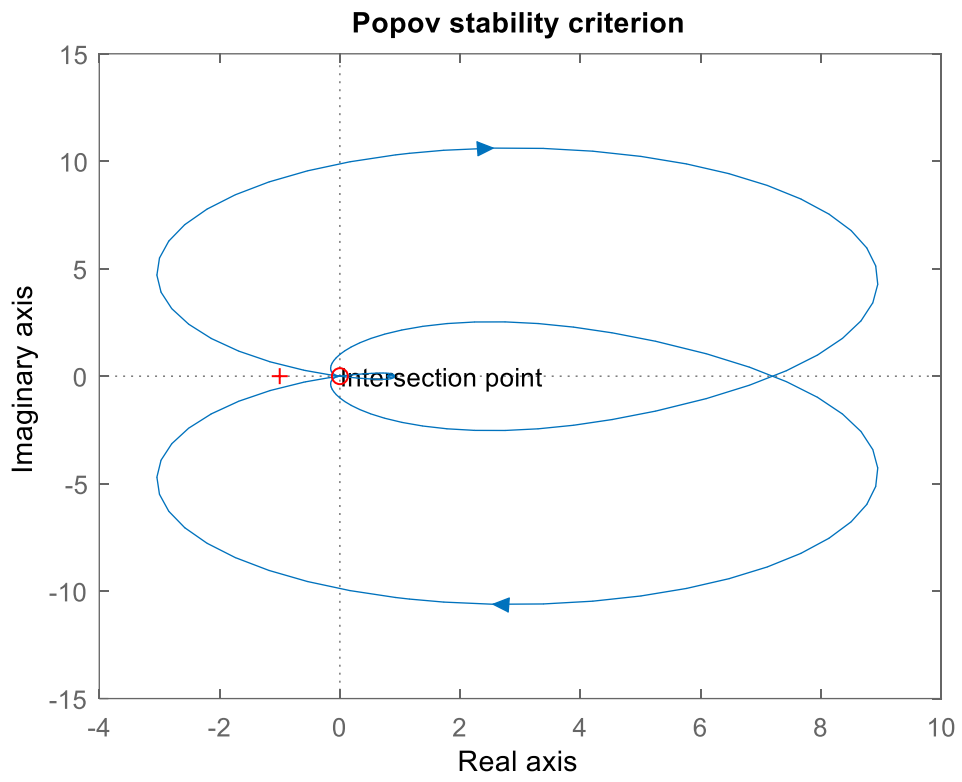


Figure 3.9 Popov Stability Criterion.

CHAPTER FOUR

4 RESULTS AND DISCUSSION

Step into the world of advanced vehicle dynamics with our cutting-edge simulation of quarter car dynamics, powered by the renowned MATLAB/SIMULINK software and based on a precise mathematical model. The simulation offers a comprehensive evaluation of the suspension system, exploring both ride comfort and car handling, while utilizing road disturbance as the input for the dynamic system. By providing crucial data on key performance indicators such as suspension travel, wheel load, and body acceleration for both passive and active suspension systems, our simulation represents an essential tool in optimizing vehicle performance. And with the vehicle traveling at varying speeds between 20km/hr to 80km/hr, our simulation provides valuable insights into the behavior of the system across a range of speeds, enabling you to make informed decisions and unlock the full potential of your vehicle.

To showcase the effectiveness of our developed methods, this chapter presents numerical simulation results. Using a simulation-based approach, we implement active control algorithms such as PID and NPID, leveraging the power of MATLAB/SIMULINK to bring our vision to life. Our focus is on the performance of the suspension system in terms of ride comfort and vehicle handling. To validate our dynamic model, we simulate the performance of both passive and active suspension systems under different road conditions and passenger car speeds. The outcome of our simulation provides valuable insights into the suspension system's behavior, unlocking the full potential of your vehicle.

Our investigation into the effect of control centers around dynamic tire compression, which serves as a powerful indicator of vehicle handling capability, and the sprung mass (chassis) position, which reflects ride comfort. Using state control variables of the system, including the vehicle's body displacement, velocity, and acceleration, as well as the unsprung mass of the front and rear wheels' heave displacement, we conduct our suspension performance analysis on the dynamic MATLAB/SIMULINK platform. Our findings showcase the active electromagnetic suspension system's remarkable ability to control the system's state to the

equilibrium position, utilizing a fast response dynamic system to enhance both passengers ride comfort and vehicle handling

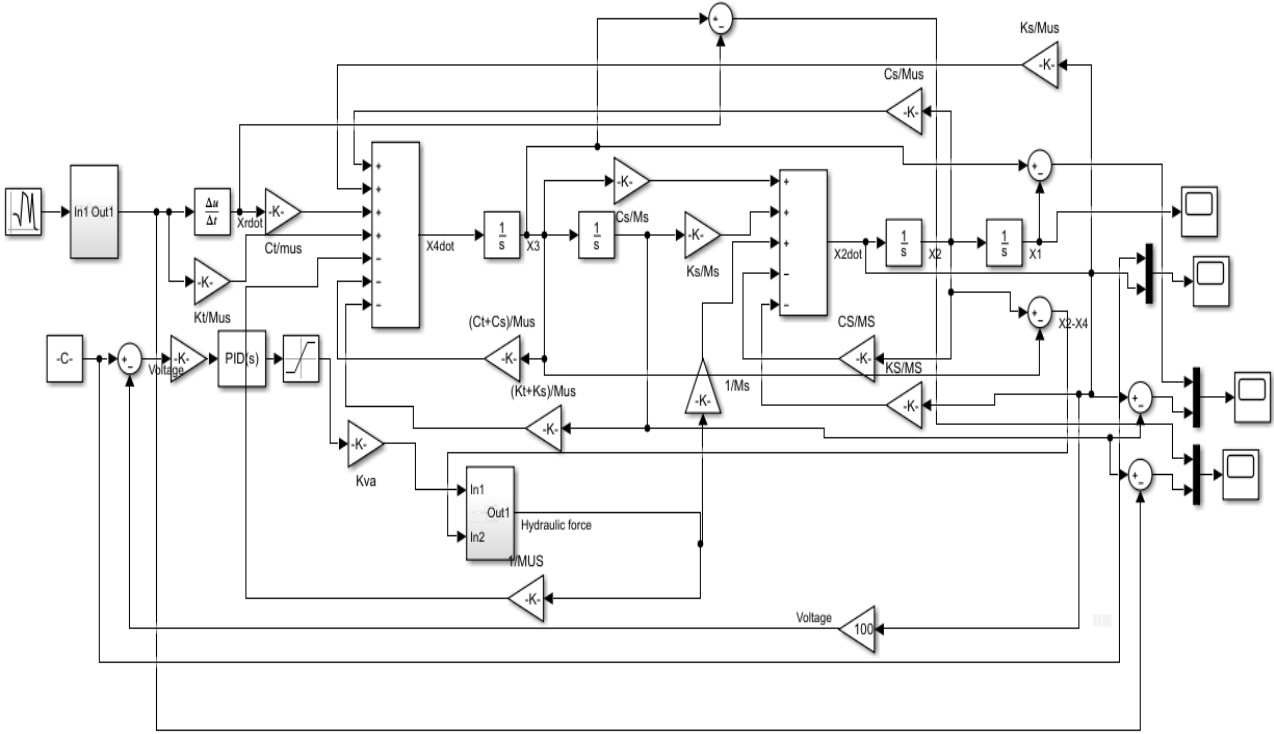


Figure 4.1 Simulation model for active quarter car suspension.

4.1 Simulation for validation of the vehicle suspension model

The study investigates the conventional stiffness and simple damper between the chassis of the sprung mass and the unsprung mass of the wheel, taking into account only tire stiffness. The simulation on a road profile reveals that the displacement of the system propagates non-uniformly, exposing the suspension system to potential damage from different road inputs. To achieve optimal vehicle handling and ride quality, our findings suggest that a controller is essential, as it extends the vehicle's life and smoothens the system with minimal steady-state errors. By implementing a controller, we can ensure the suspension system's longevity while enhancing the overall performance of the vehicle.

4.1.1 Performance analysis on the suspension system with NPID controller

Join us as we delve into a stimulating analysis and discussion section, where we explore the position and acceleration of both passive and active suspension systems, presenting our findings in an easy-to-understand visual format with a net plotted graph using MATLAB/SIMULINK. The research offers valuable insights into the behavior of the suspension systems, providing a comprehensive understanding of their performance.

4.2 Two pump sinusoidal road input disturbance

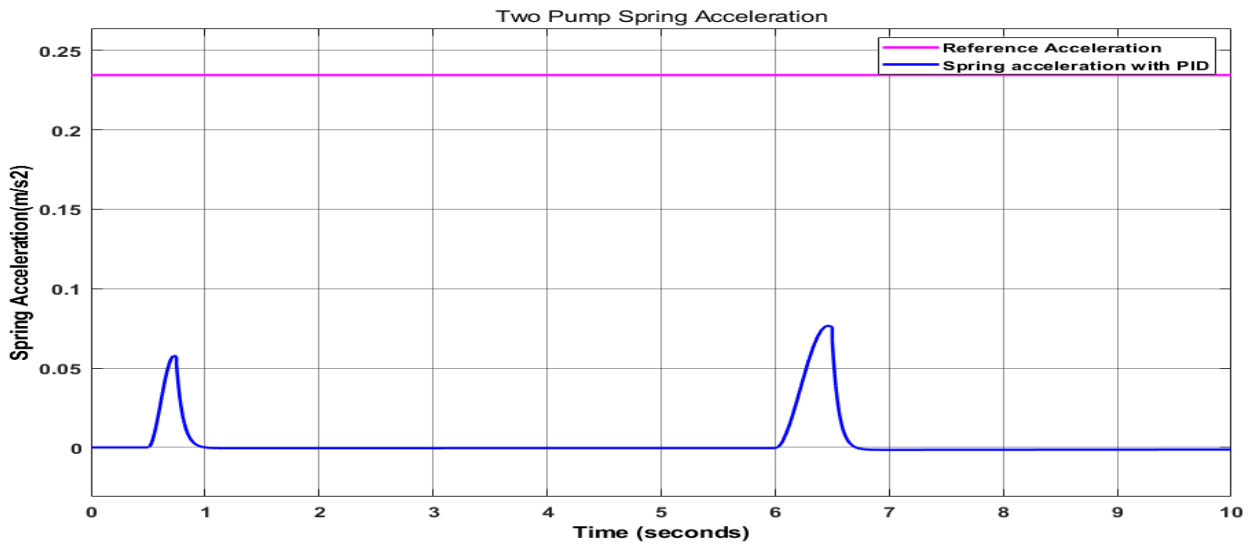


Figure 4.2 Two Pump Spring Acceleration with NPID controller.

In Figure 4.2, the graph illustrates a significant decrease in spring acceleration from the reference values of 0.2375 to an improved value of 0.08 m, thanks to the implementation of the NPID controller. Notably, the system exhibits full controllability, as depicted in the figure, where minimum values are observed at each peak. This compelling evidence indicates that the NPID controller effectively enhances ride quality, leading to a smoother and more enjoyable experience.

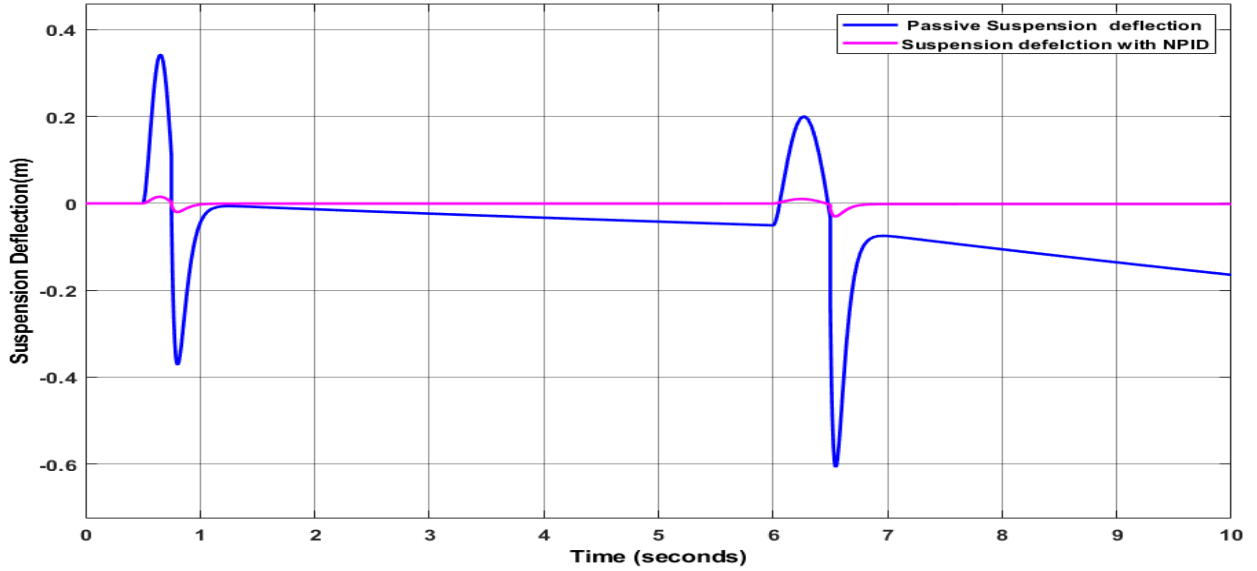


Figure 4.3 Two Pump Suspension Deflection with NPID controller.

Figure 4.3 demonstrate that remarkable performance of suspension deflection, comparing a passive suspension system with a NPID controller. Our findings reveal an astounding reduction in peak-to-peak values, with the NPID controller minimizing the peak value from 0.37 m to a mere 0.02 m in the positive peak direction. In the negative peak value direction, the PID controller's response is even more impressive, reducing the value from 0.6 m to 0.02 m by adapting to the suspension system's changes based on the NPID controller gain. Our research highlights the powerful capabilities of a NPID controller in enhancing the performance of suspension systems, unlocking the full potential of your vehicle.

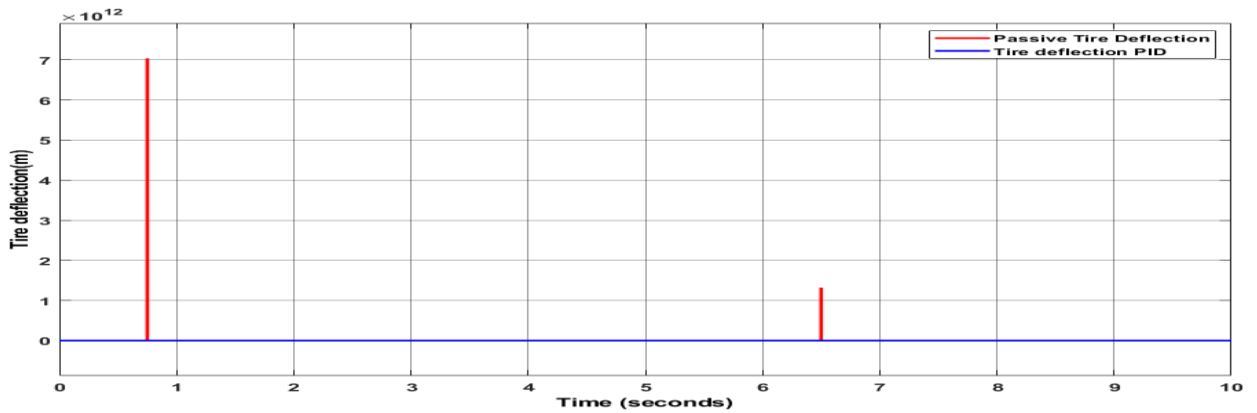


Figure 4.4 Two Pump Tire Deflection with and without NPID Controller.

Figure 4.4, where we showcase a fascinating discovery that contradicts the displacement of the Tire deflection, comparing a passive suspension system with a NPID controller. The research reveals an impressive reduction in peak-to-peak values, with the NPID controller minimizing the peak value from a staggering 7m to a remarkable 0.0m in the positive peak direction and in the negative peak direction from 0.49m to 0.015m changes. The findings illuminate the immense potential of a NPID controller in optimizing the performance of suspension systems, revolutionizing the way we approach vehicle handling and ride quality.

Table 4.1: Comparison of peak to peak under two pumps

Parameters	Peak to peak passive	Peak to peak ASS	Remark
Spring Acceleration (m/s ²)	0.2375	0.08	66.31%
Suspension Deflection(m)	0.97	0.04	95.87%
Tire Deflection(m)	7	0	100%

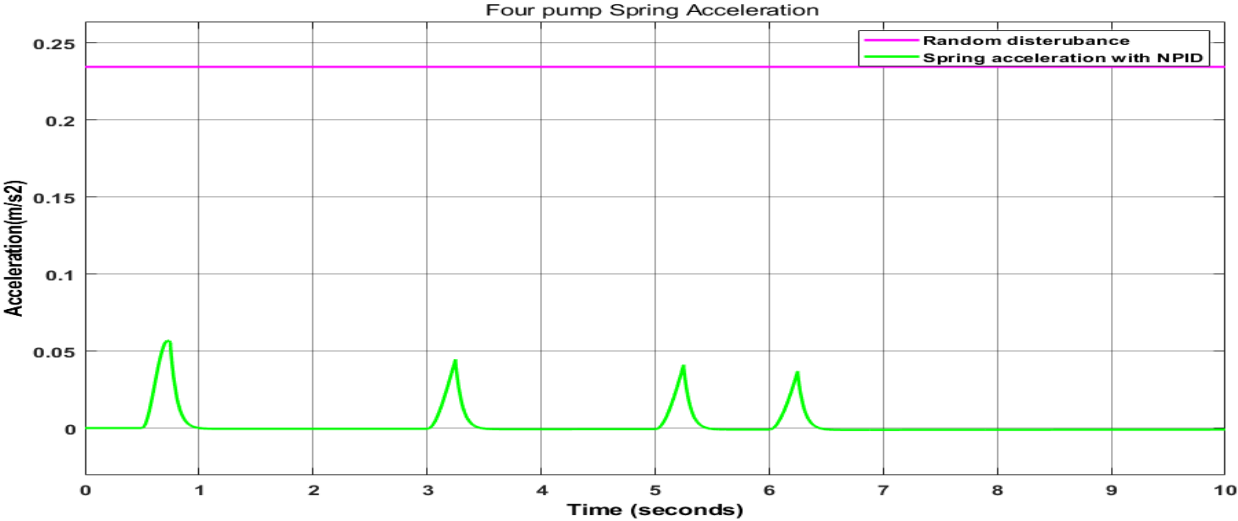


Figure 4.5 Four Pump Spring Acceleration with and without NPID Controller.

4.3 Four pump sinusoidal road input Disturbance

In Figure 4.5, the graph illustrates a significant decrease in spring acceleration from the reference value of 0.2375 to an improved value of 0.052 m, thanks to the implementation of the NPID controller. Notably, the system exhibits full controllability, as depicted in the figure,

where minimum values are observed at each peak. This compelling evidence indicates that the NPID controller effectively enhances ride quality, leading to a smoother and more enjoyable experience

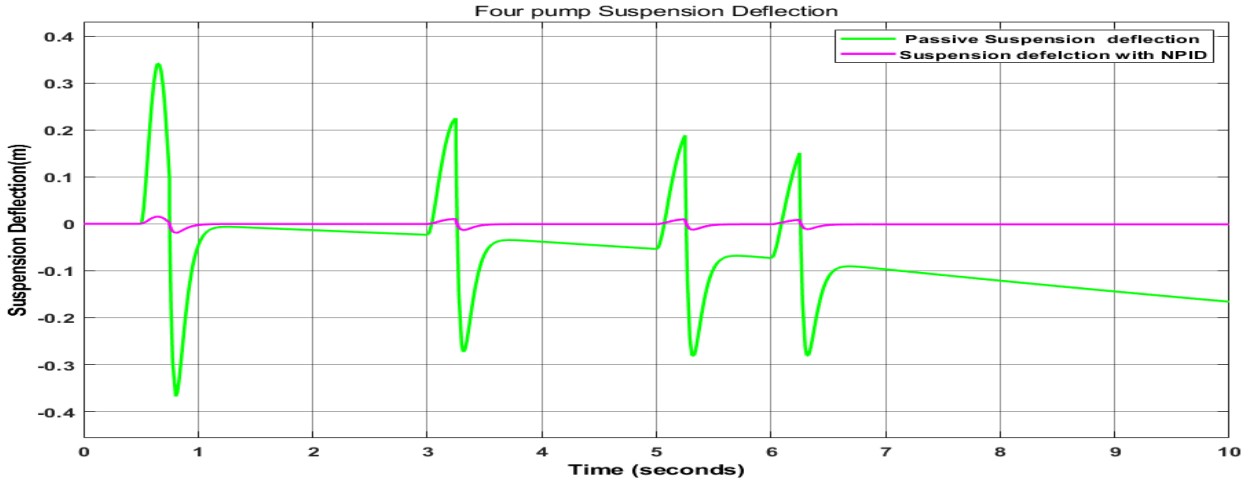


Figure 4.6 Four Pump Suspension Deflection with and without NPID Controller.

Figure 4.6, where we present groundbreaking findings that challenge the displacement of the suspension deflection, comparing a passive suspension system with a NPID controller. The research uncovers a substantial reduction in peak-to-peak values, with the NPID controller minimizing the peak value from 0.345 m to 0.015 m in the positive peak direction. Even more impressive is the NPID controller's response in the negative peak value direction, reducing the value from 0.38 m to 0.015 m by dynamically adapting to the suspension system's changes based on the NPID controller gain. The research highlights the unparalleled potential of a NPID controller in optimizing suspension system performance, revolutionizing the way we approach ride quality and vehicle handling.

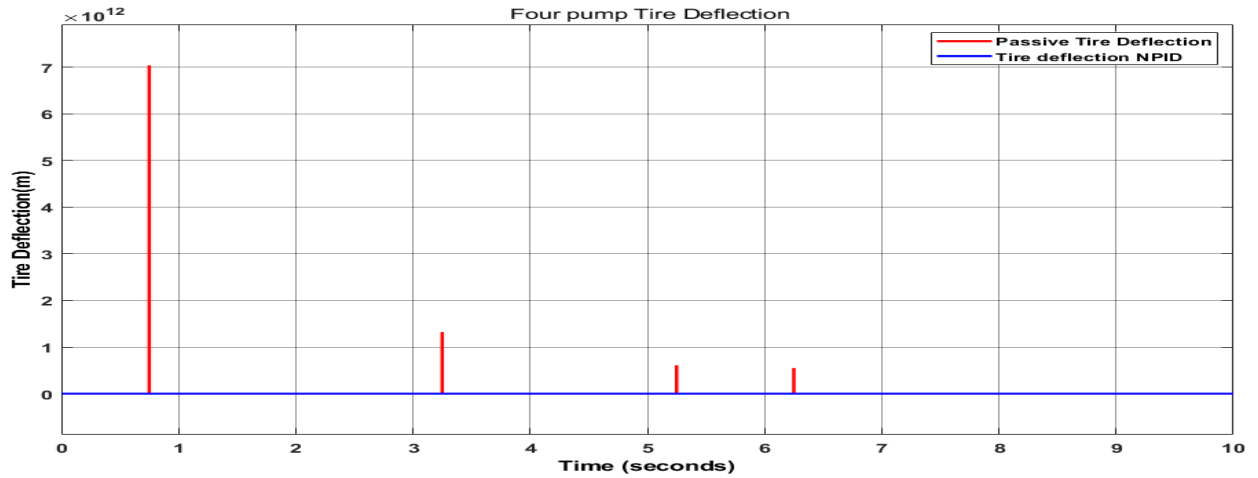


Figure 4.7 Four Pump Tire Deflection with and without NPID Controller.

Figure 4.7 where we showcase a fascinating discovery that contradicts the displacement of the tire deflection, comparing a passive suspension system with a NPID controller. The research reveals an impressive reduction in peak-to-peak values, with the NPID controller minimizing the peak value from a staggering 7.0m to a remarkable 0.0m in the positive peak direction. The findings illuminate the immense potential of a NPID controller in optimizing the performance of suspension systems, revolutionizing the way we approach vehicle handling and ride quality.

Table 4.2: Comparison of peak to peak under four pump

Parameters	Peak to peak passive	Peak to peak ASS	Remark
Spring Acceleration (m/s ²)	0.2375	0.052	66.31%
Suspension Deflection(m)	0.725	0.03	95.86%
Tire Deflection(m)	7	0	100%

4.4 Simulation Results of Type A random road input at Four different vehicle speeds

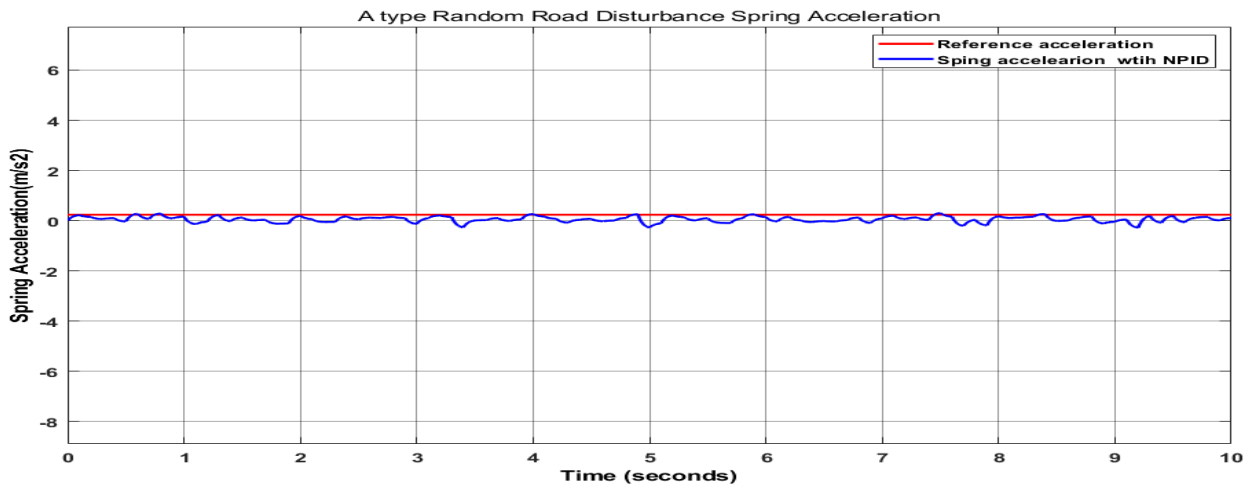


Figure 4.8 A Type Random Road Disturbance Spring Acceleration at 20km/hr.

Figure 4.8 presents a compelling contradiction between the reference acceleration of the spring mass and the acceleration achieved with a NPID controller. Notably, the peak-to-peak value comparison of the NPID controller closely matches the peak value, remaining at 0.2375m in the positive peak direction. However, in the negative peak value direction, the NPID controller exhibits a more substantial reduction, reaching 0.2m. This significant difference underscores the NPID controller's capability to respond to changes in spring acceleration, thereby influencing the overall acceleration profile.

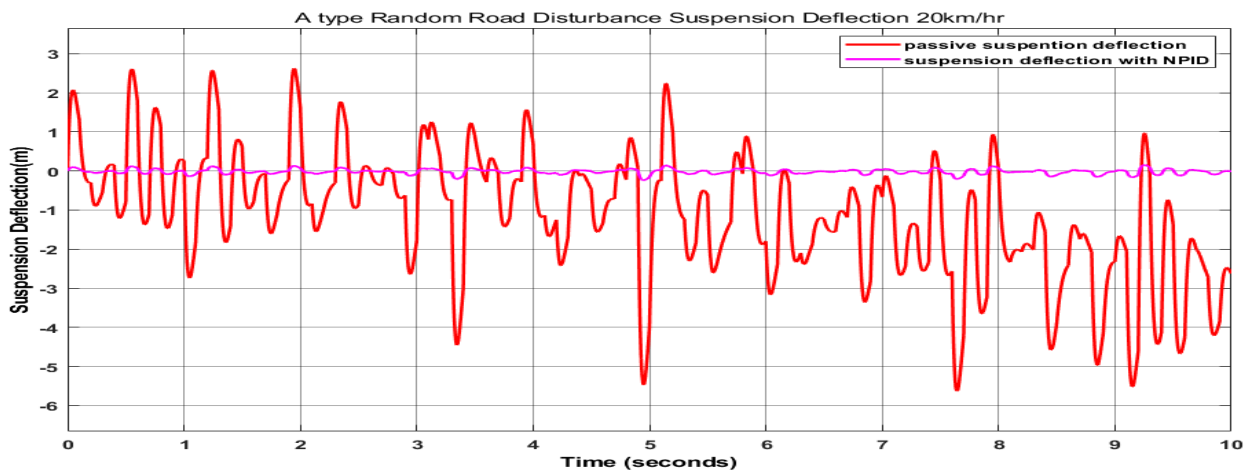


Figure 4.9A type Random Road Disturbance Suspension Deflection at 20km/hr.

Figure 4.9, spring suspension deflection, comparing a passive suspension system with a NPID controller. The research showcases an impressive reduction in peak-to-peak values, with the NPID controller minimizing the peak value from 2.7 m to 0.15 m in the positive peak direction. The NPID controller's response in the negative peak value direction is even more impressive, reducing the value from 5.5 m to 0.15 m by dynamically adapting to the suspension system's changes based on the NPID controller gain. The research underscores the immense potential of a NPID controller in optimizing suspension system performance, revolutionizing the way we approach ride quality and vehicle handling.

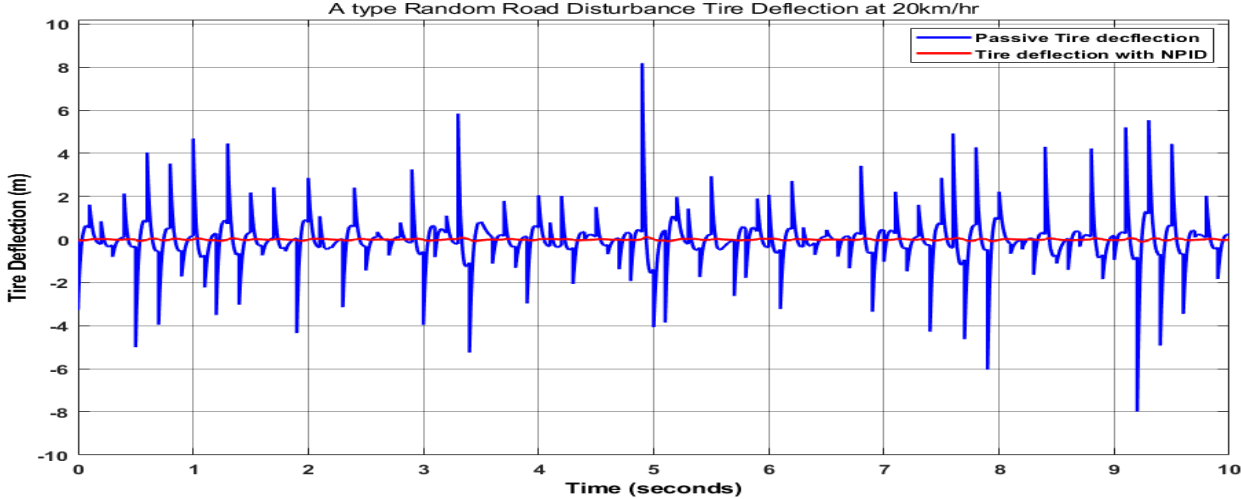


Figure 4.10 A type Random Road Disturbance Tire Deflection at 20m/hr.

Figure 4.10 which show cases groundbreaking findings that challenge the displacement of the chassis at tire deflection, comparing a passive suspension system with a NPID controller. The research highlights an impressive reduction in peak-to-peak values, with the NPID controller minimizing the peak value from a staggering 8.5m to a remarkable 0.15 m in the positive peak direction. The NPID controller's response in the negative peak value direction is even more remarkable, reducing the value from 8 m to 0.15 m by dynamically adapting to the suspension system's changes based on the NPID controller. The research unlocks the full potential of a NPID controller in optimizing suspension system performance, revolutionizing the way we approach vehicle handling and ride quality.

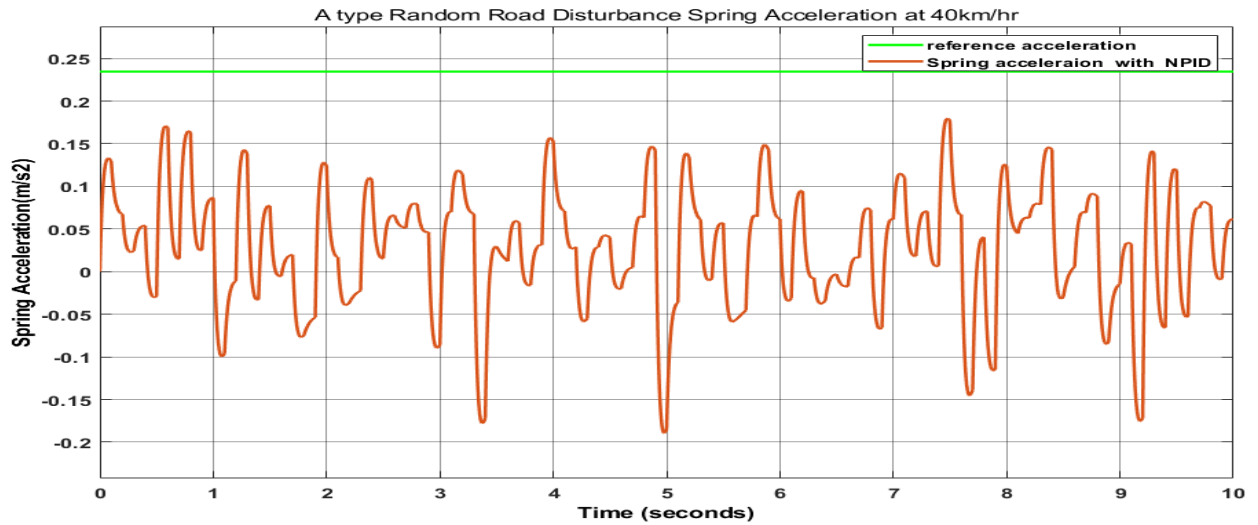


Figure 4.11 A type Random Road Disturbance Spring Acceleration at 40km/hr.

Figure 4.11 unveils a compelling contradiction between the spring acceleration reference and the acceleration achieved with a NPID controller. Upon analysis, it is evident that the peak-to-peak value comparison of the NPID controller results in a reduction of the peak value, decreasing from 0.2375m to 0.175m in the positive peak direction. Conversely, in the negative peak value direction, the NPID controller exhibits a more significant reduction, reaching 0.19m. This notable disparity highlights the NPID controller's ability to respond to changes in spring acceleration and effectively influence the overall acceleration profile.

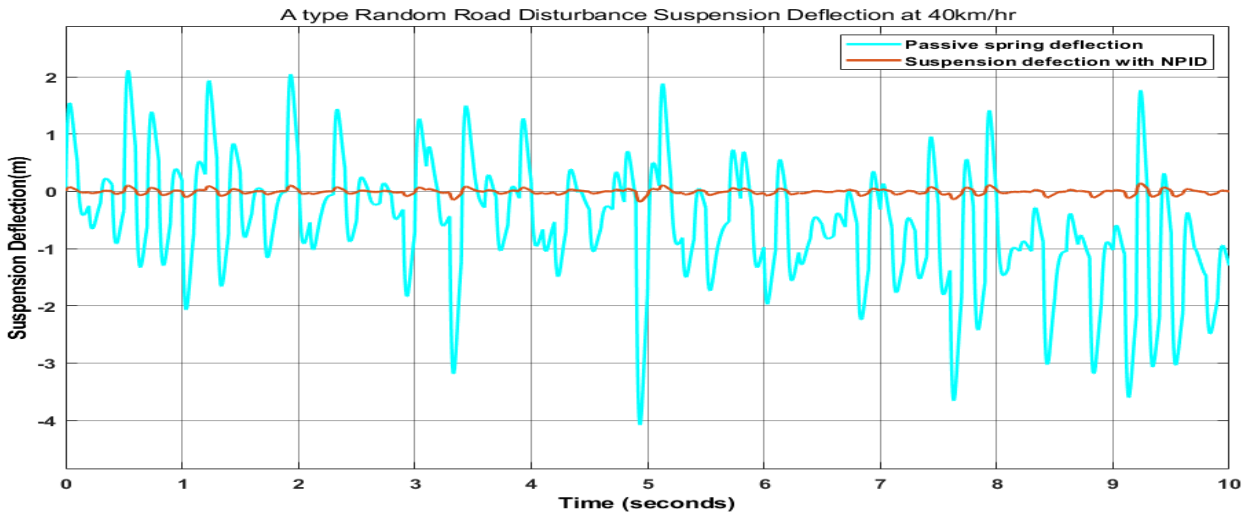


Figure 4.12 A type Random Road Disturbance Spring Deflection at 40km/hr.

Figure 4.12, which reveals groundbreaking findings that challenge the displacement of the suspension deflection, comparing a passive suspension system with a NPID controller. The research demonstrates an impressive reduction in peak-to-peak values, with the NPID controller minimizing the peak value from 2.1 m to a mere 0.15 m in the positive peak direction. The NPID controller's response in the negative peak value direction is even more remarkable, reducing the value from 4.1 m to 0.15 m by dynamically adapting to the suspension system's changes based on the NPID controller gain. The research highlights the immense potential of a NPID controller in optimizing suspension system performance, revolutionizing the way we approach ride quality and vehicle handling.

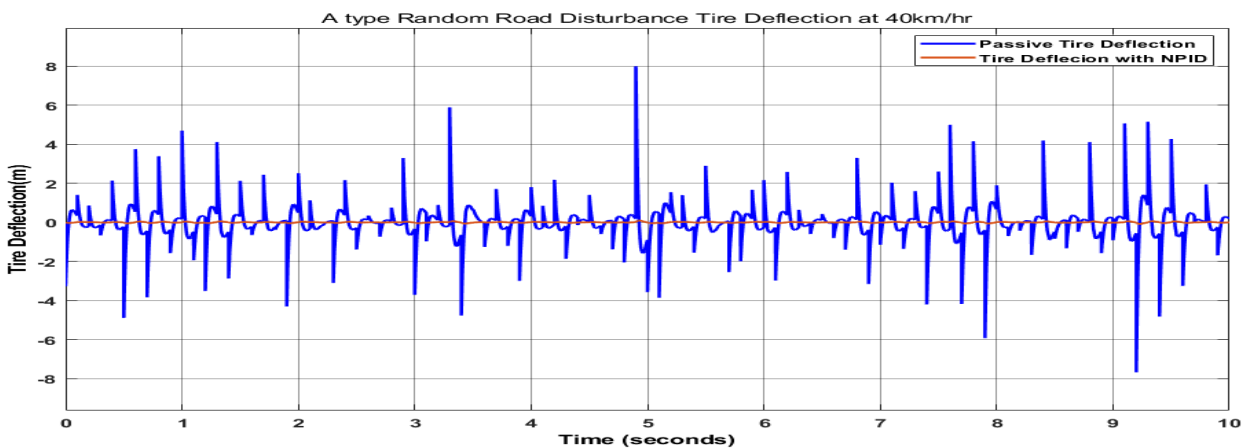


Figure 4.13 A type Random Road Disturbance Tire Deflection at 40km/hr.

Figure 4.13, which unveils groundbreaking findings that challenge the displacement of tire deflection, comparing a passive suspension system with a NPID controller. The research demonstrates an impressive reduction in peak-to-peak values, with the NPID controller minimizing the peak value from a staggering 8.0 m to an astonishing 0.15 m in the positive peak direction. The NPID controller's response in the negative peak value direction is even more remarkable, reducing the value from 7.9m to 0.15 m by dynamically adapting to the suspension system's changes based on the NPID controller gain. The research highlights the immense potential of a NPID controller in optimizing suspension system performance, revolutionizing the way we approach vehicle handling and ride quality.

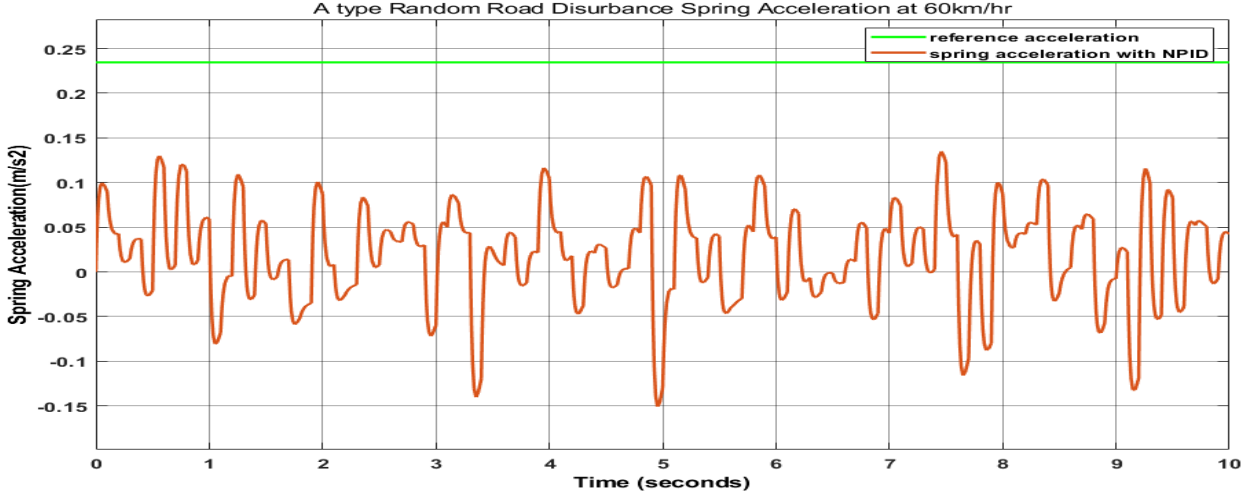


Figure 4.14 A type Random Road Disturbance Spring Acceleration at 60km/hr.

Figure 4.14 unveils a striking contradiction to the Reference Acceleration when employing a NPID controller. Notably, the peak-to-peak value comparison of the NPID controller leads to a reduction in the peak value, diminishing from 0.2375m to 1.3m in the positive peak direction. Conversely, in the negative peak value direction, the NPID controller exhibits a more pronounced reduction, amounting to 0.149m. This substantial difference underscores the NPID controller's ability to respond to variations in spring acceleration and effectively influence the overall acceleration profile.

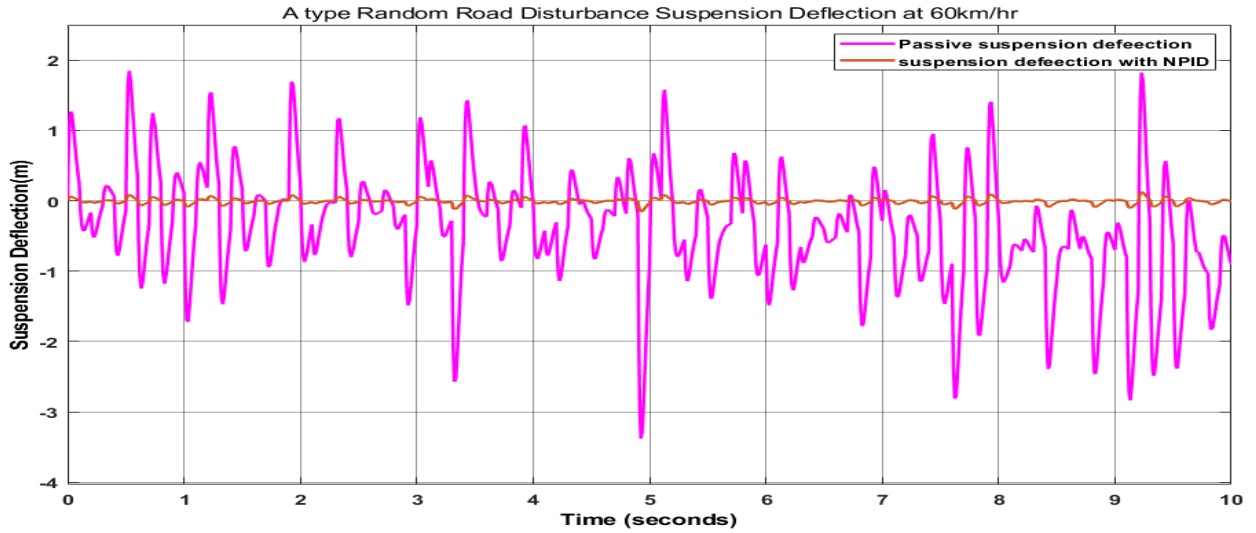


Figure 4.15 A type Random Road Disturbance Suspension Deflection at 60km/hr.

Figure 4.15, which presents groundbreaking findings that challenge the displacement of the at spring suspension deflection, comparing a passive suspension system with a NPID controller. The research showcases an impressive reduction in peak-to-peak values, with the NPID controller minimizing the peak value from 1.8 m to 0.15 m in the positive peak direction. The NPID controller's response in the negative peak value direction is even more remarkable, reducing the value from 3.4 m to 0.15 m by dynamically adapting to the suspension system's changes based on the NPID controller gain. The research highlights the immense potential of a NPID controller in optimizing suspension system performance, unlocking the full potential of your vehicle's handling and ride quality.

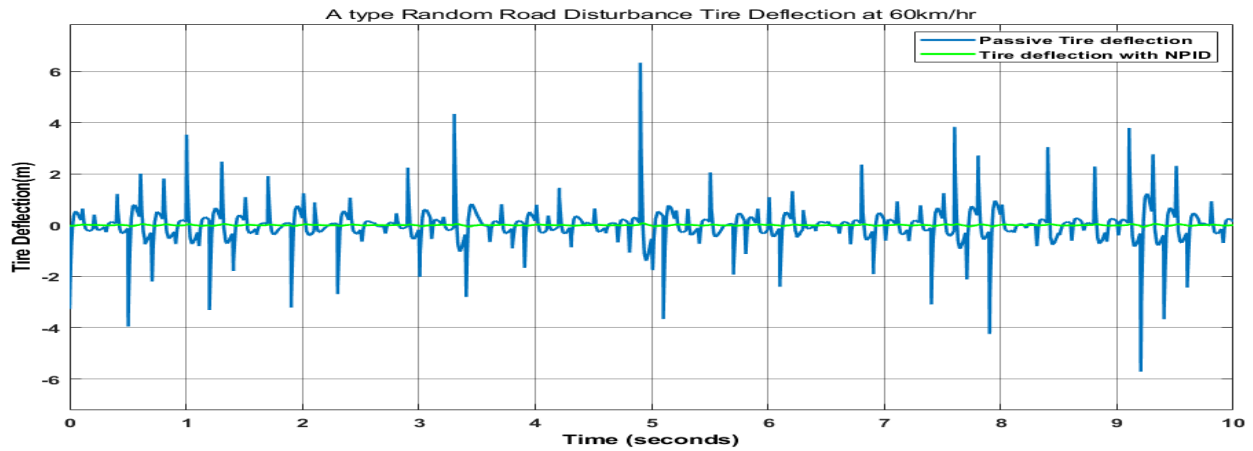


Figure4.16 A type Random Road Disturbance Tire Deflection at 60km/hr.

Figure 4.16, which unveils groundbreaking findings that challenge the displacement of the tire deflection, comparing a passive suspension system with a NPID controller. The research showcases an impressive reduction in peak-to-peak values, with the NPID controller minimizing the peak value from a staggering 6.4m to a remarkable 0.2 m in the positive peak direction. The NPID controller's response in the negative peak value direction is even more remarkable, reducing the value from 5.9 m to 0.2 m by dynamically adapting to the suspension system's changes based on the PID controller gain. The research highlights the immense potential of a NPID controller in optimizing suspension system performance, revolutionizing the way we approach vehicle handling and ride quality.

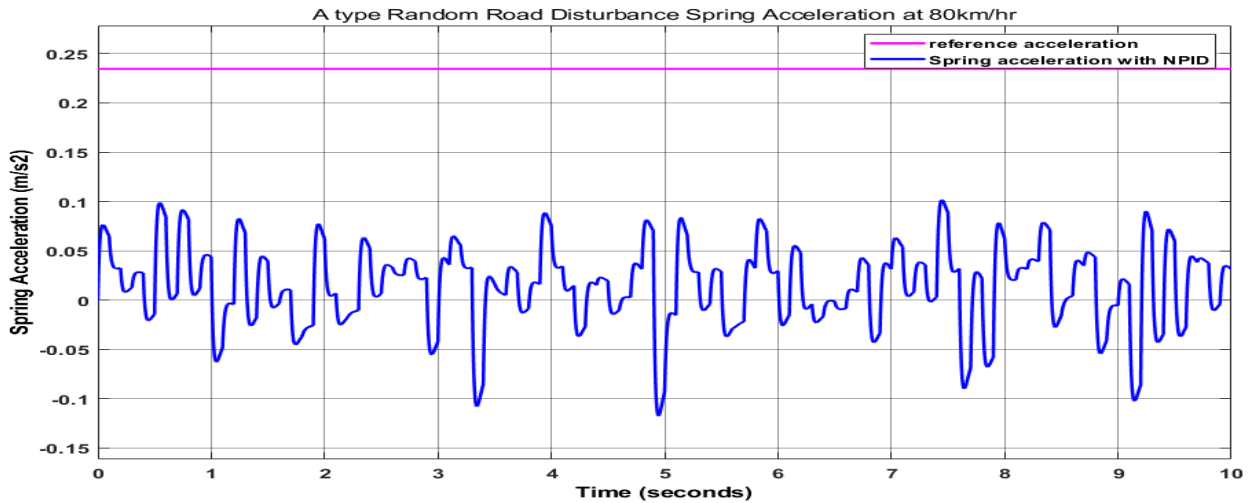


Figure 4.17 A type Random Road Disturbance Spring Acceleration at 80km/hr.

Figure 4.17 presents a compelling contrast between the reference acceleration and the acceleration obtained using a NPID controller. Notably, the peak-to-peak value comparison of the NPID controller results in a reduction of the peak value, decreasing from 0.2373m to 0.1m in the positive peak direction. Conversely, in the negative peak value direction, the NPID controller exhibits a more substantial reduction, amounting to 0.12m. This discrepancy highlights the NPID controller's capacity to respond to changes in spring acceleration, thereby contributing to the observed variations in the acceleration profile.

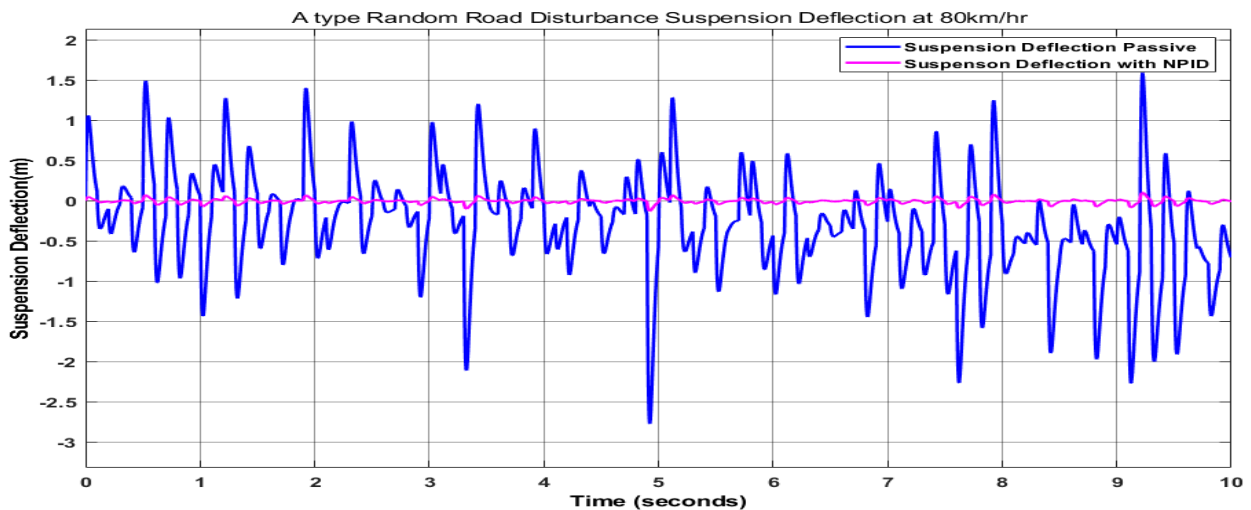


Figure 4.18 A type Random Road Disturbance suspension deflection at 80km/hr.

Figure 4.18, which presents groundbreaking findings that challenge spring suspension deflection, comparing a passive suspension system with a NPID controller. The research showcases an impressive reduction in peak-to-peak values, with the NPID controller minimizing the peak value from 1.6 m to a mere 0.1 m in the positive peak direction. The NPID controller's response in the negative peak value direction is simply astonishing, reducing the value from a staggering 2.75 m to 0.1 m by dynamically adapting to the suspension system's changes based on the NPID controller gain. The research highlights the immense potential of a NPID controller in optimizing suspension system performance, revolutionizing the way we approach vehicle handling and ride quality.

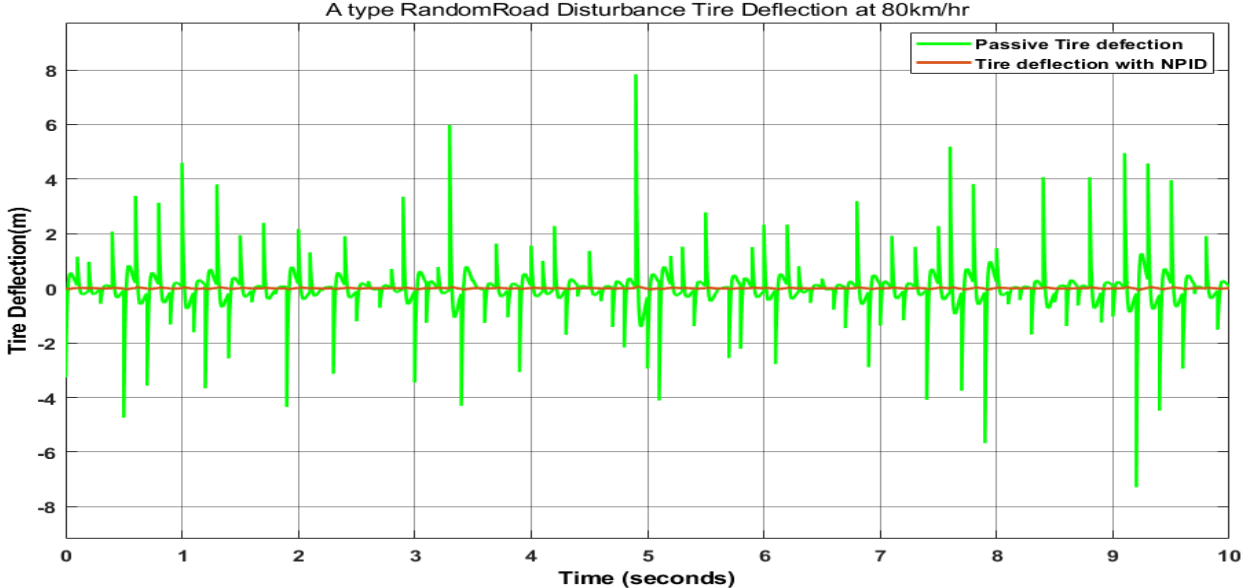


Figure 4.19 A type Random Road Disturbance Tire Deflection at 80km/hr.

Figure 4.19, which presents groundbreaking findings that challenge the displacement of the tire deflection, comparing a passive suspension system with a NPID controller. The research showcases an impressive reduction in peak-to-peak values, with the NPID controller minimizing the peak value from a staggering 7.9 m to a remarkable 0.1 m in the positive peak direction. The NPID controller's response in the negative peak value direction is even more impressive, reducing the value from 7.5 m to 0.1m by dynamically adapting to the suspension system's changes based on the NPID controller gain. The research highlights the immense potential of a NPID controller in optimizing suspension system performance, unlocking the full potential of your vehicle's handling and ride quality.

Table 4.3: peak to peak values of PSS using type A random input simulation

Parameters	Peak to peak PSS 20km/hr	Peak to peak PSS 40km/hr	Peak to Peak PSS 60km/hr	Peak to Peak PSS 80km/hr
Spring Acceleration (m/s ²)	0.2375	0.2375	0.2375	0.2375
Suspension Deflection(m)	8.2	6.2	5.2	4.35
Tire Deflection(m)	16.5	15.9	12.3	15.4

Table 4.4: peak to peak values of ASS using type A random input simulation

Parameters	Peak to peak ASS 20km/hr	Peak to peak ASS 40km/hr	Peak to Peak ASS 60km/hr	Peak to Peak ASS 80km/hr
Spring Acceleration(m/s ²)	0.2375	0.175	0.13	0.1
Suspension Deflection(m)	0.3	0.3	0.3	0.2
Tire Deflection(m)	0.3	0.3	0.4	0.2

4.5 Simulation Results of Type B random road input at four different vehicle speeds

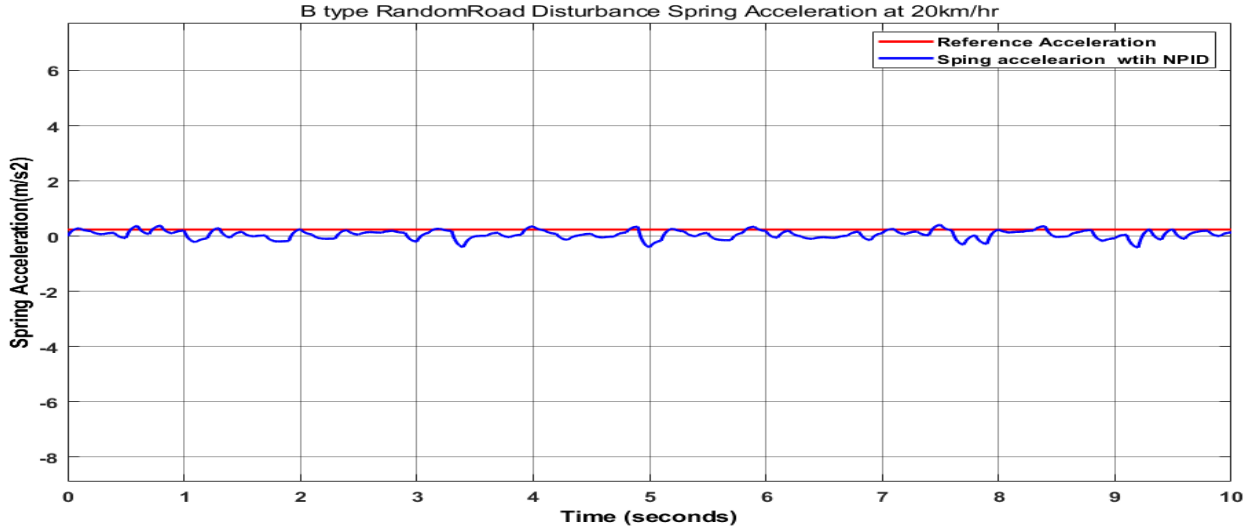


Figure 4.20 B type Random Road disturbance Spring Acceleration at 20km/hr.

Figure 4.20 reveals a contradiction between the reference acceleration and the acceleration achieved with a NPID controller. Upon closer examination, it is observed that the peak-to-peak value comparison of the NPID controller closely matches the peak value, transitioning from 0.2375m to 0.2376m in the positive peak direction. Conversely, in the negative peak value direction, the NPID controller exhibits a more significant reduction, reaching 0.5m. This notable discrepancy can be attributed to the NPID controller's ability to respond to changes in spring acceleration, which is influenced by the NPID controller gain.

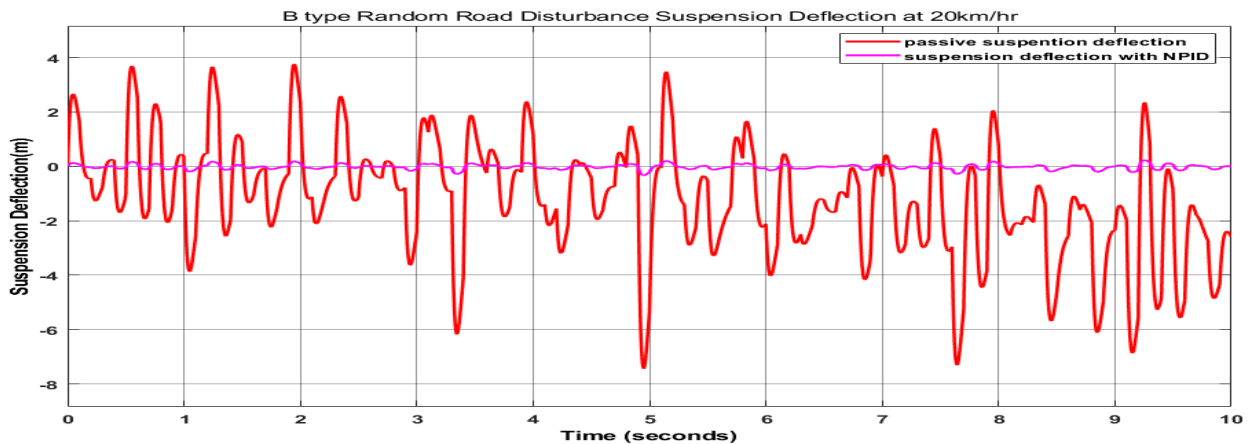


Figure 4.21 B type Random Road Disturbance Suspension Deflection at 20km/hr.

Figure 4.21, which reveals groundbreaking findings that challenge the displacement of the spring suspension deflection, comparing a passive suspension system with a NPID controller. The research showcases an impressive reduction in peak-to-peak values, with the NPID controller minimizing the peak value from 3.8 m to 0.2 m in the positive peak direction. The NPID controller's response in the negative peak value direction is even more remarkable, reducing the value from 7.6 m to 0.2 m by dynamically adapting to the suspension system's changes based on the NPID controller gain. Our research highlights the immense potential of a NPID controller in optimizing suspension system performance, revolutionizing the way we approach vehicle handling and ride quality.

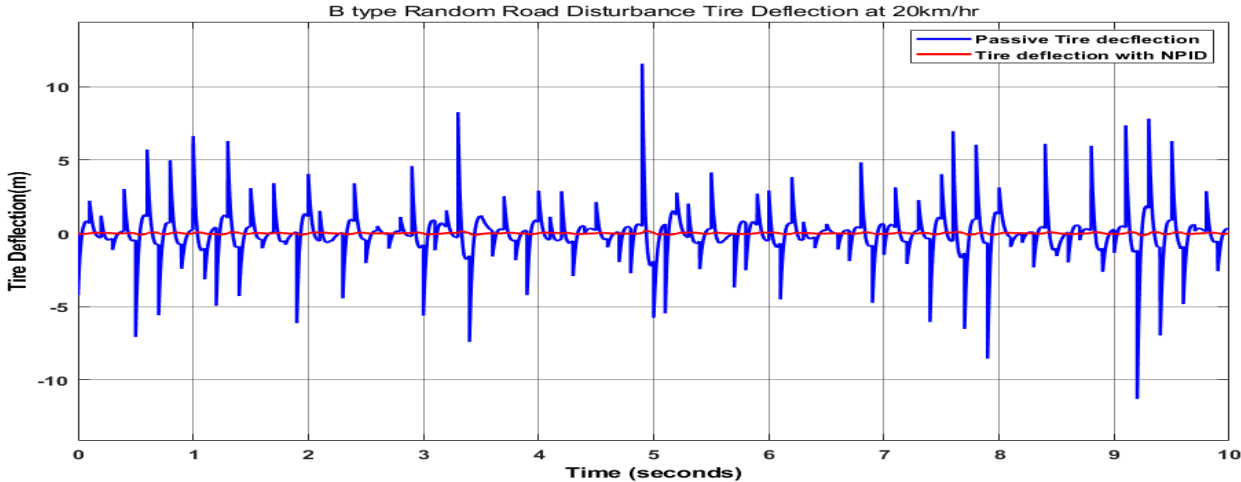


Figure 4.22 B type Random Road Disturbance Tire Deflection at 20km/hr.

Figure 4.22, which present groundbreaking findings that challenge the spring deflection suspension, comparing a passive suspension system with a NPID controller. The research showcases an impressive reduction in peak-to-peak values, with the NPID controller minimizing the peak value from a whopping 12.5m to 0.25 m in the positive peak direction. The NPID controller's response in the negative peak value direction is even more remarkable, reducing the value from 12.5 m to 0.25 m by dynamically adapting to the suspension system's changes based on the NPID controller gain. The research highlights the immense potential of a NPID controller in optimizing suspension system performance, unlocking the full potential of your vehicle's handling and ride quality.

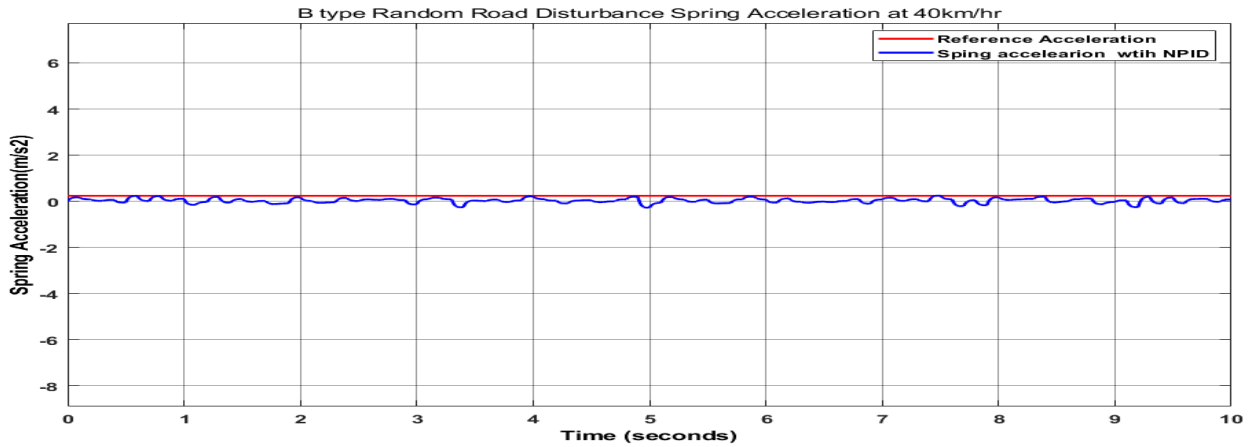


Figure 4.23 B type Random Road Disturbance Spring Acceleration at 40km/hr.

Figure 4.23 presents a compelling contradiction to the reference acceleration when utilizing a NPID controller. Upon analysis, it is observed that the peak-to-peak value comparison of the NPID controller matches the peak value, remaining at 0.2375m in the positive peak direction. However, in the negative peak value direction, the NPID controller exhibits a more substantial reduction, reaching 0.2375m. This demonstrates the NPID controller's responsiveness to changes in the suspension system, facilitated by the adjustable NPID controller gain.

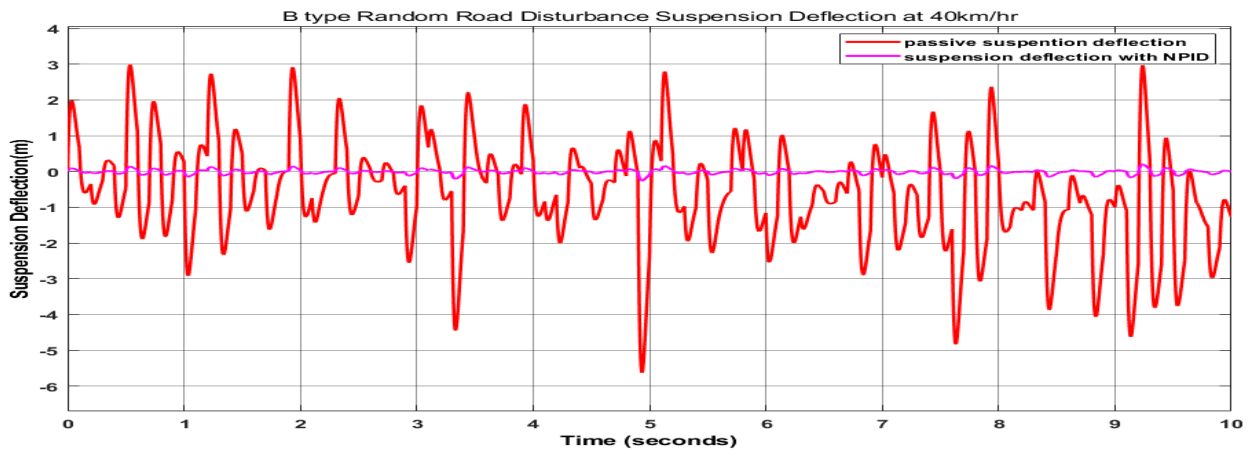


Figure 4.24 B type Random Road Disturbance Suspension Deflection at 40km/hr.

Figure 4.24 shows that contradict the displacement of the spring suspension deflection passive with a NPID controller. In this case, the peak-to-peak value comparison of the NPID controller reduces the peak value from 3 m to 0.2 m in the positive peak direction. Whereas in the negative peak value direction, the NPID controller shows a higher value reduction (5.6 to

0.2) by giving a response to the change of the suspension system based on the NPID controller gain.

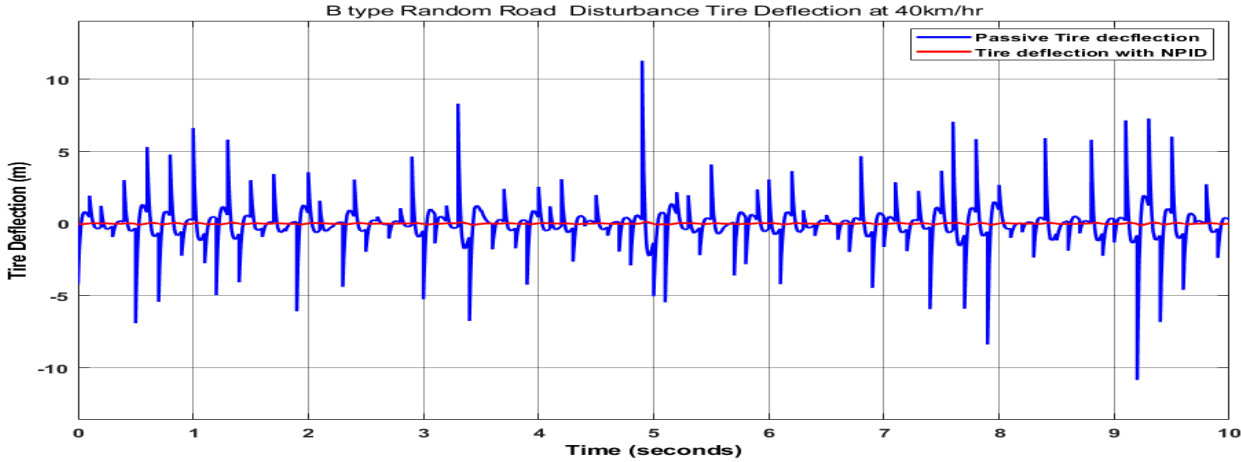


Figure 4.25 B type Random Road Disturbance Tire Deflection at 40km/hr.

A figure 4.25 show that contradicts the displacement of the tire deflection is a passive with a controller NPID. In this case, the peak-to-peak value comparison of the NPID controller reduces the peak value from 12m to 0.25 m in the positive peak direction. Whereas in the negative peak value direction, the NPID controller shows a higher value reduction (11 to 0.25m) by giving a response to the change of the suspension system based on the NPID controller gain.

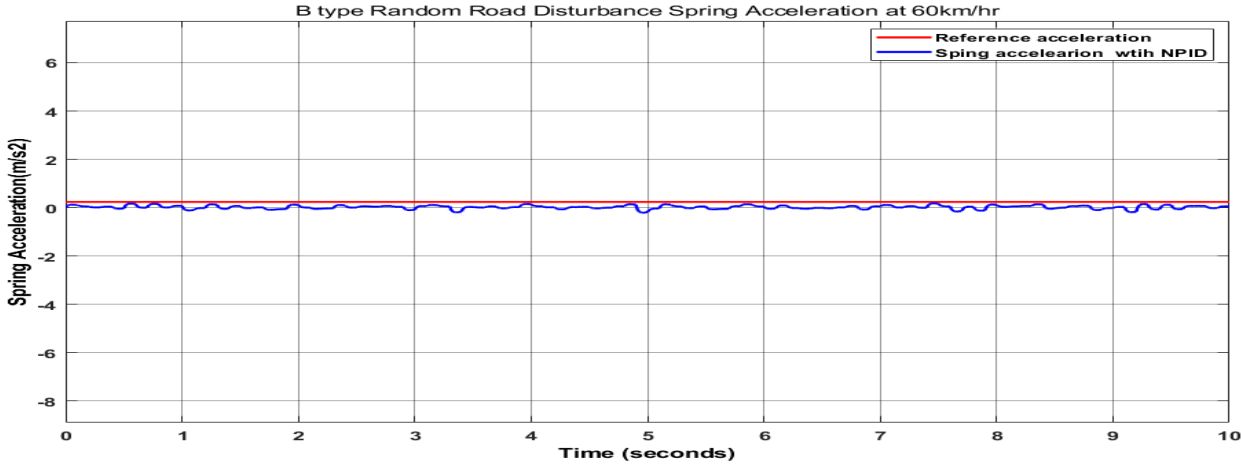


Figure 4.26 B type Random Road Disturbance Spring Acceleration at 60km/hr.

Figure 4.26 reveals a striking contradiction between the reference acceleration and the acceleration achieved with a NPID controller. Notably, the peak-to-peak value comparison of the NPID controller results in a reduction of the peak value, diminishing from 0.2375m to 0.237m in the positive peak direction. Conversely, in the negative peak value direction, the NPID controller exhibits a more pronounced reduction, amounting to 0.23m. This substantial difference underscores the NPID controller's ability to respond to changes in spring acceleration and significantly influence the overall acceleration profile.

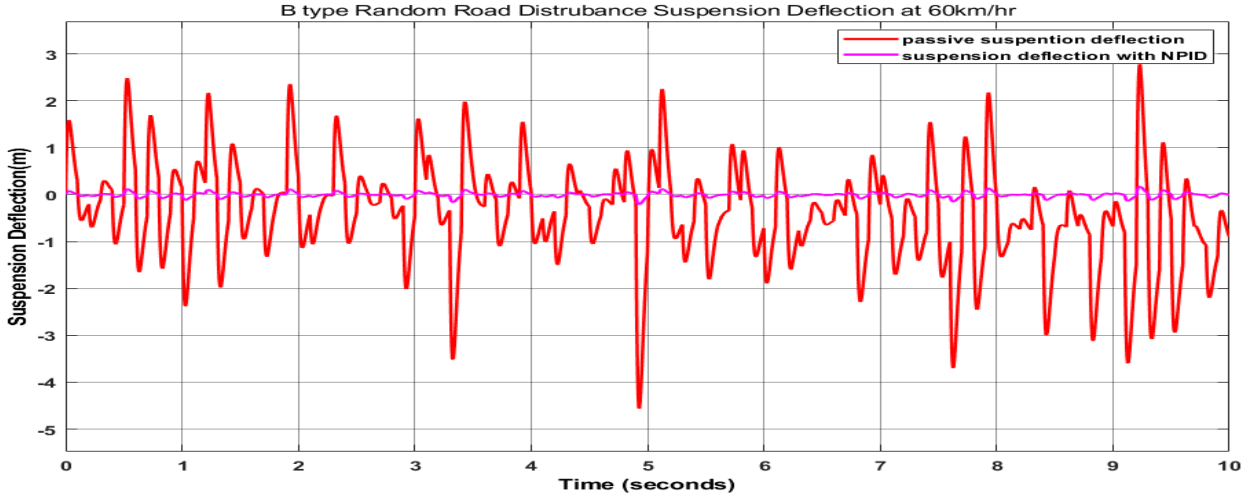


Figure 4.27 B type Random Road Disturbance Suspension Deflection at 60km/hr.

A figure 4.27 show that contradicts the displacement of the suspension deflection is a passive with NPID controller. In this case, the peak-to-peak value comparison of the NPID controller reduces the peak value from 2.8 m to 0.1 m in the positive peak direction. Whereas in the negative peak value direction, the NPID controller shows a higher value reduction (4.5 to 0.1) by giving a response to the change of the suspension system based on the NPID controller gain.

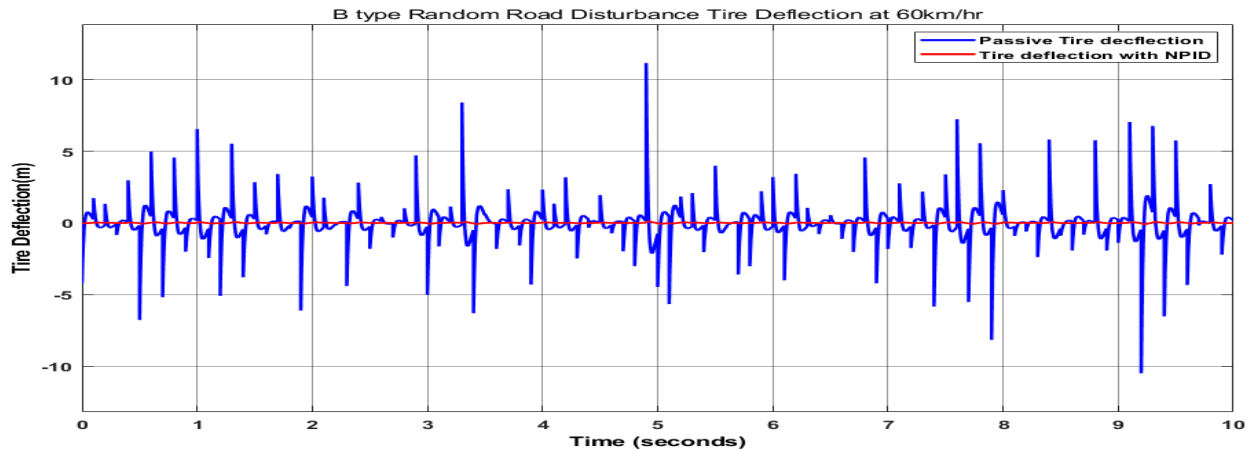


Figure 4.28 B type Random Road Disturbance Tire Deflection at 60km/hr.

Figure 4.28 shows that contradict the displacement of the chassis at the tire deflection passive with a NPID controller. In this case, the peak-to-peak value comparison of the NPID controller reduces the peak value from 12m to 0.2 m in the positive peak direction. Whereas in the negative peak value direction, the NPID controller shows a higher value reduction (11m to 0.2m) by giving a response to the change of the suspension system based on the NPID controller gain

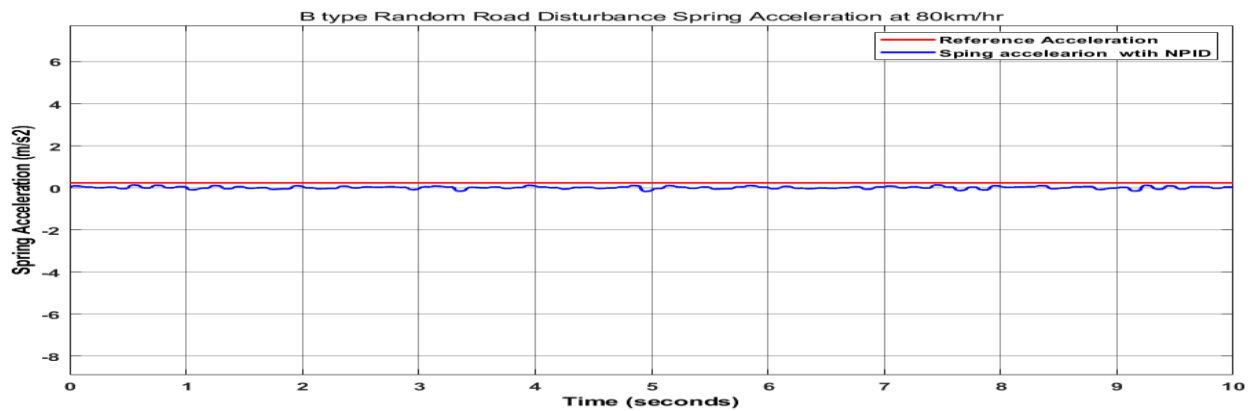


Figure 4.29 B type Random Road Disturbance Spring Acceleration at 80m/hr.

Figure 4.29 exhibits a compelling contradiction between the reference acceleration and the acceleration achieved with a NPID controller. Upon examination, it is evident that the peak-to-peak value comparison of the NPID controller leads to a reduction in the peak value, decreasing from 0.2375m to 0.23m in the positive peak direction. Conversely, in the negative

peak value direction, the NPID controller demonstrates a more significant reduction, amounting to 0.2m. This noteworthy disparity is a result of the NPID controller's response to changes in the suspension system, driven by the adjustable NPID controller gain.

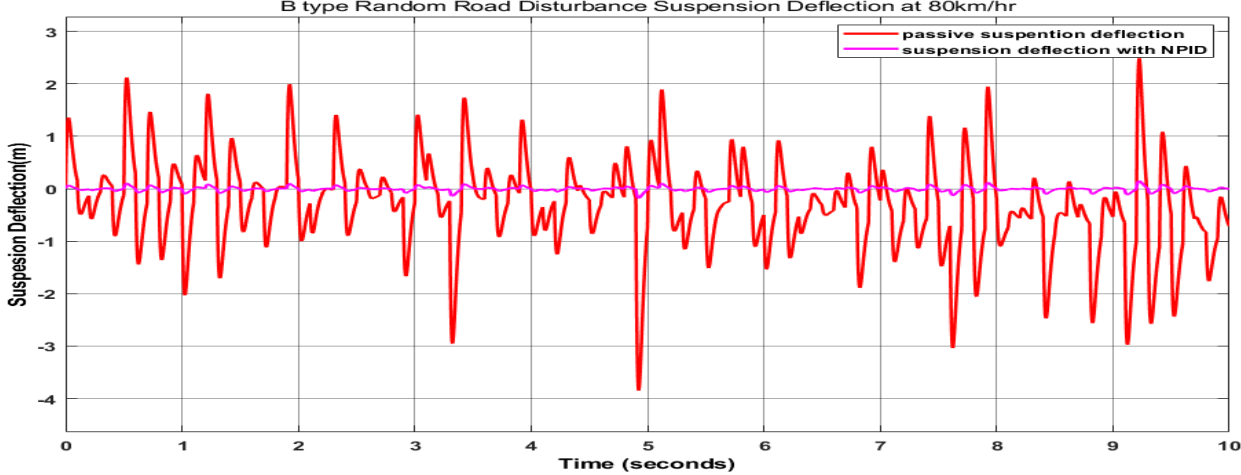


Figure 4.30 B type Random Road Disturbance Suspension Deflection at 80km/hr.

A figure 4.30 show that contradicts the displacement of the suspension deflection is a passive with a controller NPID. In this case, the peak-to-peak value comparison of the NPID controller reduces the peak value from 2.6m to 0.15 m in the positive peak direction. Whereas in the negative peak value direction, the NPID controller shows a higher value reduction (3.9 to 0.15) by giving a response to the change of the suspension system based on the NPID controller gain.

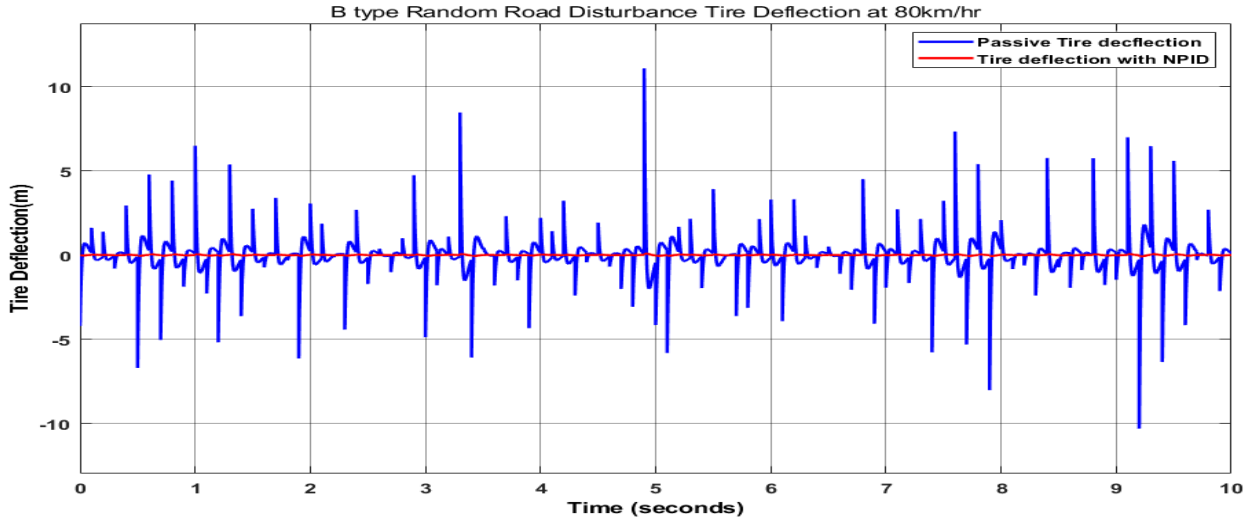


Figure 4.31 B type Random Road Disturbance Tire Deflection at 80km/hr.

A figure 4.31 show that contradicts the displacement of the tire deflection is a passive with a NPID controller. In this case, the peak-to-peak value comparison of the NPID controller reduces the peak value from 12 m to 0.2 m in the positive peak direction. Whereas in the negative peak value direction, the NPID controller shows a higher value reduction (10.5to 0.2m) by giving a response to the change of the suspension deflection based on the NPID controller gain.

Table 4.5: peak to peak values of PSS using type B random road input simulation

Parameters	Peak to peak PSS 20km/hr	Peak to peak PSS 40km/hr	Peak to Peak PSS 60km/hr	Peak to Peak PSS 80km/hr
Spring Acceleration (m/s ²)	0.2375	0.2375	0.2375	0.2375
Suspension Deflection(m)	11.4	8.6	7.3	6.5
Tire Deflection(m)	25	23	23	22.5

Table 4.6: peak to peak values of ASS using type B random road input simulations

Parameters	Peak to peak ASS 20km/hr	Peak to peak ASS 40km/hr	Peak to Peak ASS 60km/hr	Peak to Peak ASS 80km/hr
Spring Acceleration (m/s ²)	0.2375	0.2375	0.2375	0.23
Suspension Deflection(m)	0.4	0.4	0.2	0.3
Tire Deflection(m)	0.5	0.5	0.4	0.4

4.6 Simulation Results of Type C random road input at four different vehicle speeds

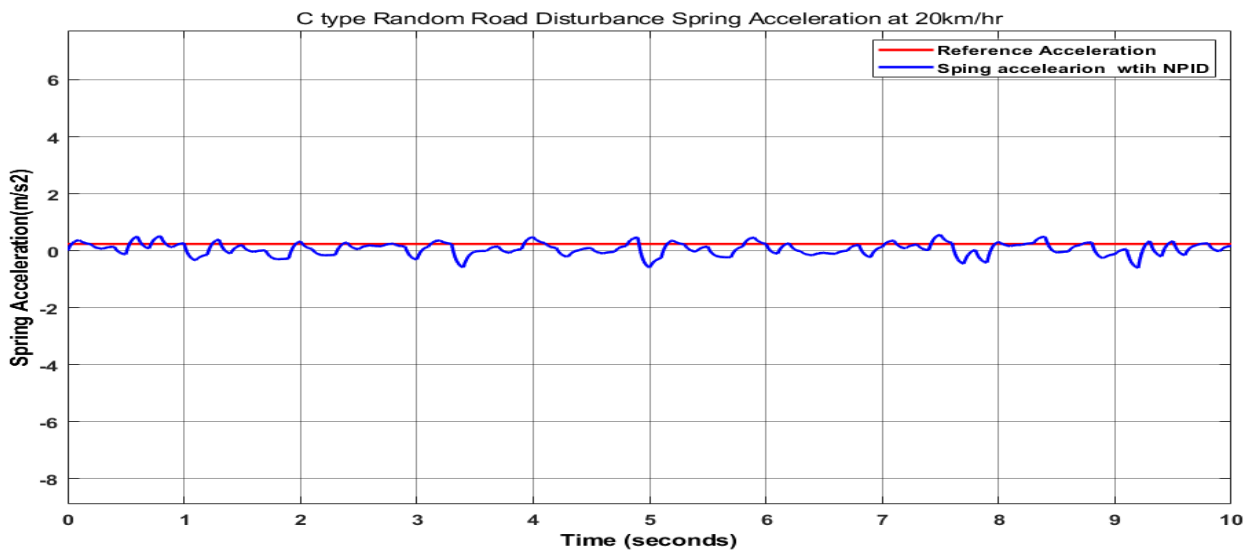


Figure 4.32 C type Random Road Disturbance Spring Acceleration at 20km/hr.

Based on the evidence presented in Figure 4.32, it can be observed that the reference acceleration contradicts the NPID controller. Specifically, when comparing the peak-to-peak values, the NPID controller almost reaches reference value the positive peak value from 0.2375 m to 0.2378 m. Conversely, in the negative peak value direction, the NPID controller exhibits a greater reduction of 0.5 m. This response is attributed to the NPID controller gain, which prompts a reaction to the suspension system's alteration.

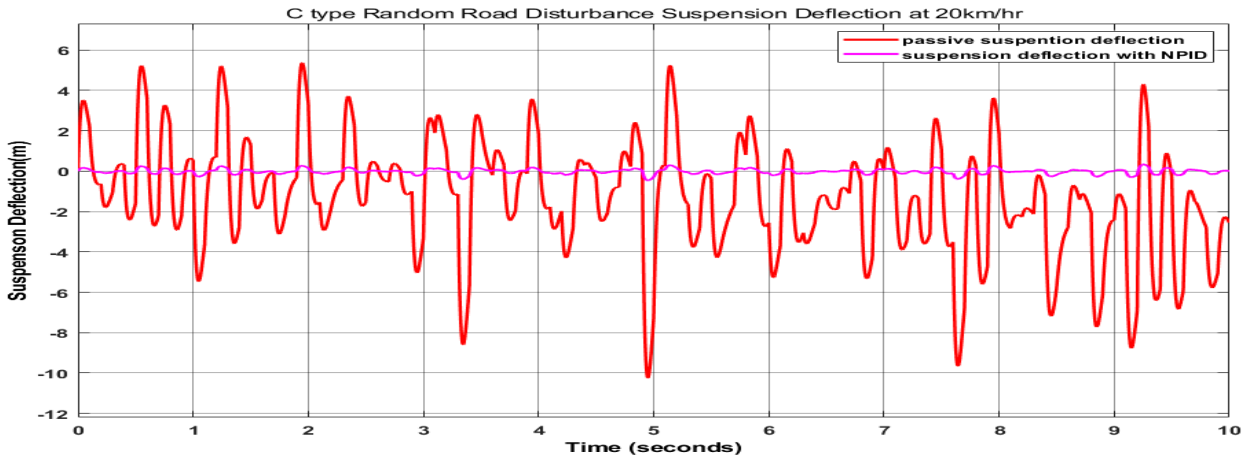


Figure 4.33 C type Random Road Disturbance Suspension Deflection at 20km/hr

A figure 4.33 show that contradicts the displacement spring suspension deflection is a passive with a NPID controller. In this case, the peak-to-peak value comparison of the NPID controller reduces the peak value from 5.5 m to 0.3 m in the positive peak direction. Whereas in the negative peak value direction, the NPID controller shows a higher value reduction (10 m to 0.3 m) by giving a response to the change of the suspension system based on the NPID controller gain.

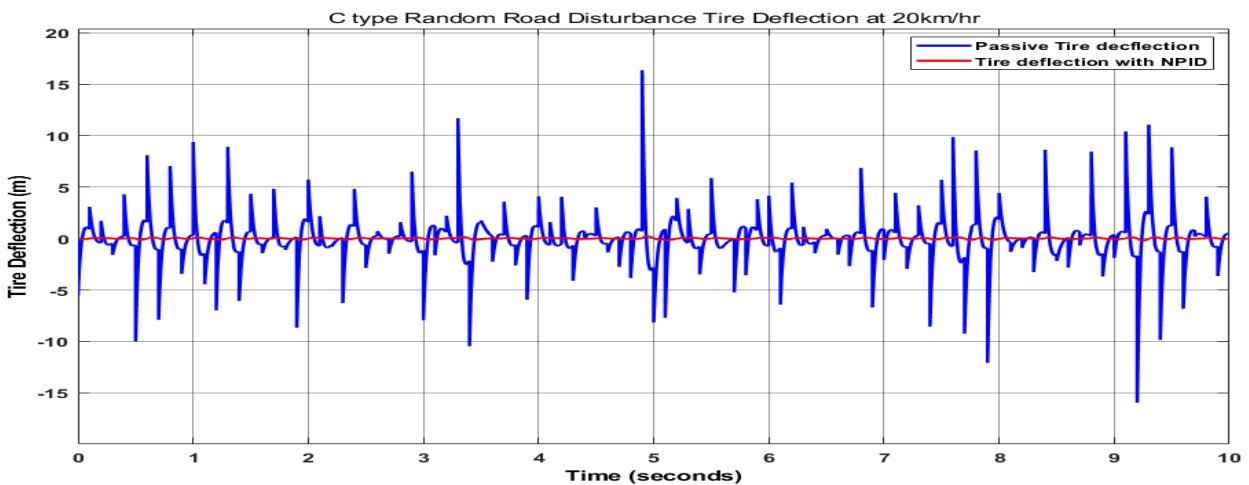


Figure 4.34 C type Random Road Disturbance Tire Deflection at 20km/hr.

A figure 4.34 show that contradicts the displacement of the tire deflection is a passive with a controller NPID. In this case, the peak-to-peak value comparison of the NPID controller reduces the peak value from 16.5m to 0.3 m in the positive peak direction. Whereas in the negative peak value direction, the NPID controller shows a

higher value reduction (16 to 0.3) by giving a response to the change of the tire deflection based on the NPID controller gain

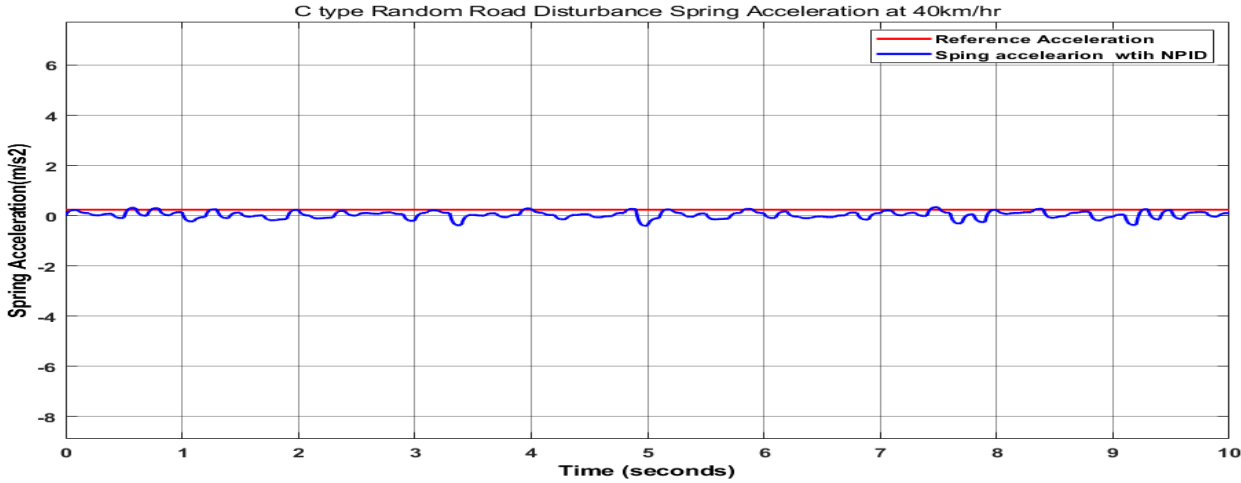


Figure 4.35 C type Random Road Disturbance Spring Acceleration at 40km/h.

Figure 4.35 shows that contradict the reference acceleration with a NPID controller. In this case, the peak-to-peak value comparison of the NPID controller reduces the peak value from 0.2375 m to 0.2375 m in the positive peak direction. Whereas in the negative peak value direction, the NPID controller shows a higher value reduction (0.237m) by giving a response to the change of the spring acceleration based on the NPID controller gain.

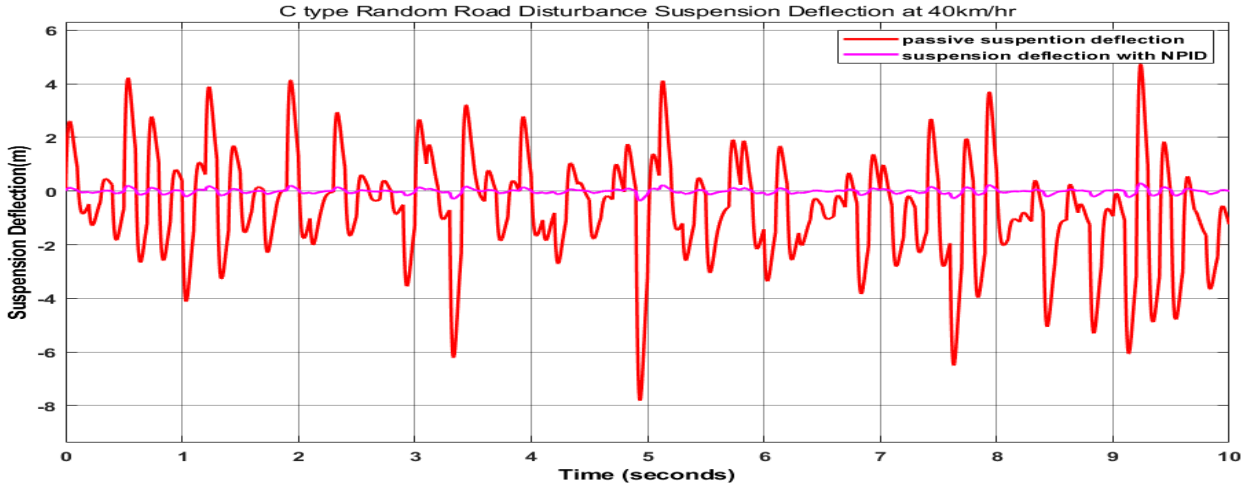


Figure 4.36 C type Random Road Disturbance Suspension Deflection at 40km/hr.

Figure 4.36 shows that contradict the displacement of the suspension deflection passive with a PID controller. In this case, the peak-to-peak value comparison of the PID controller reduces

the peak value from 5 m to 0.3 m in the positive peak direction. Whereas in the negative peak value direction, the PID controller shows a higher value reduction (7.9 m to 0.3 m) by giving a response to the change of the suspension deflection based on the PID controller gain.

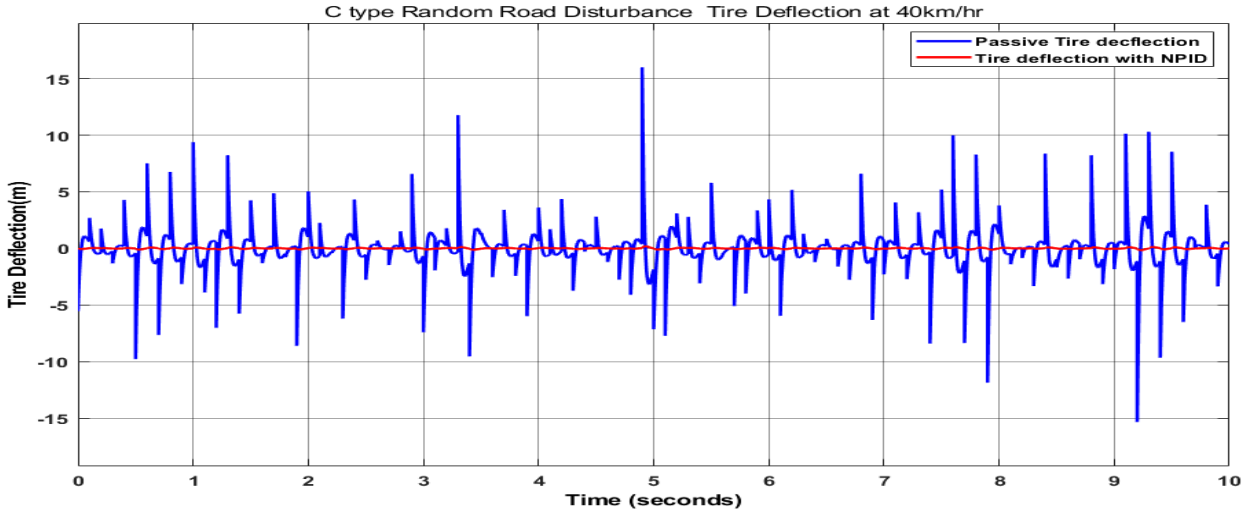


Figure 4.37 C type Random Road Disturbance Tire Deflection at 40km/hr.

A figure 4.37 show that contradicts the displacement of the tire deflection is a passive with a NPID controller. In this case, the peak-to-peak value comparison of the NPID controller reduces the peak value from 16m to 0.3 m in the positive peak direction. Whereas in the negative peak value direction, the NPID controller shows a higher value reduction (15.5 m to 0.3 m) by giving a response to the change of the tire deflection based on the NPID controller gain.

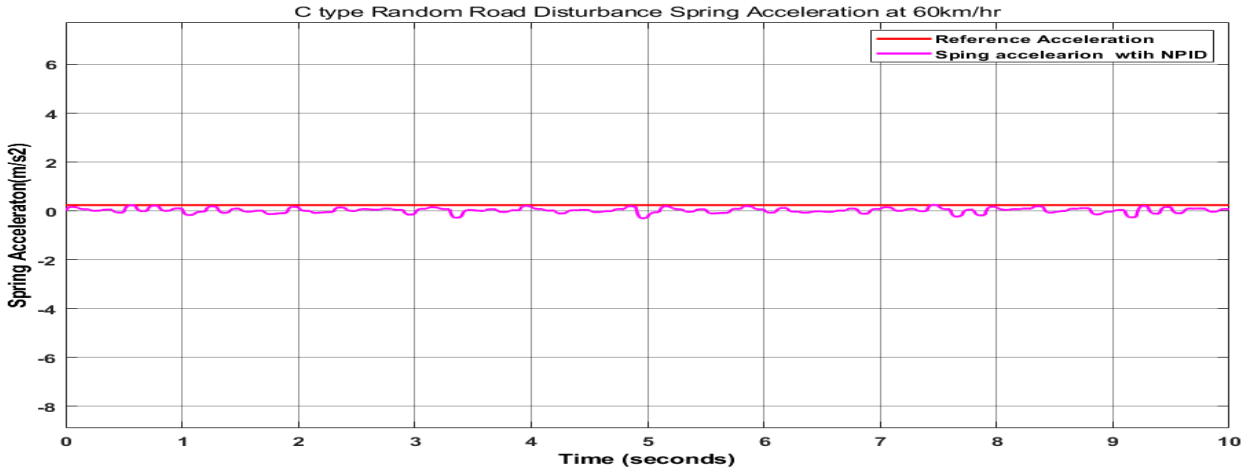


Figure 4.36 C type Random Road Disturbance Spring Acceleration at 60km/hr.

Figure 4.36 shows that contradict the reference acceleration with a NPID controller. In this case, the peak-to-peak value comparison of the NPID controller equal to the peak value from 0.2375m to 0.2375 m in the positive peak direction. Whereas in the negative peak value direction, the NPID controller shows a higher value reduction (0.2375m) by giving a response to the change of the spring acceleration.

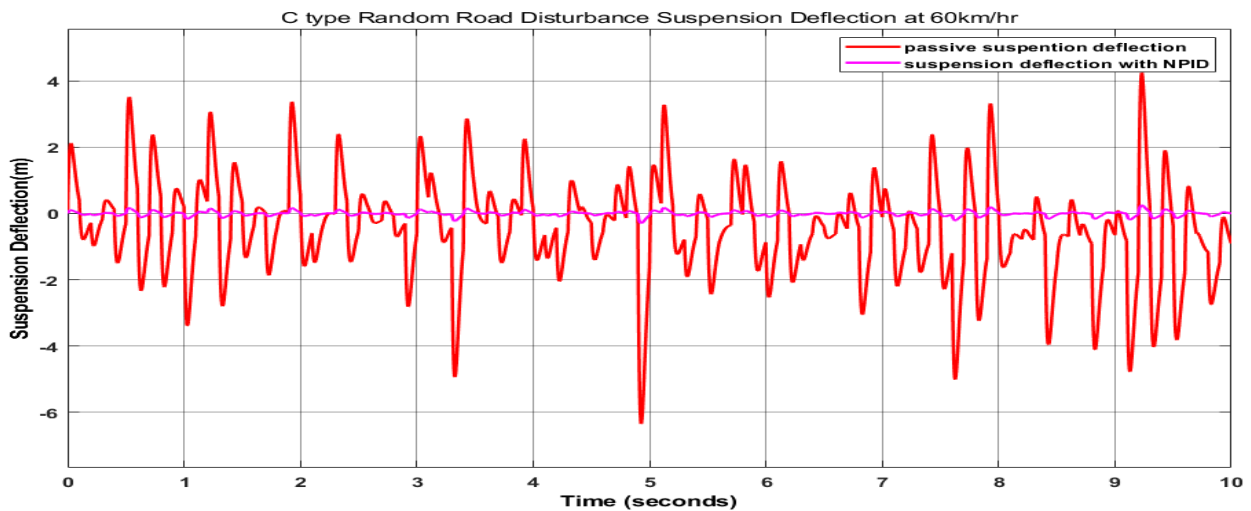


Figure 4.37 C type Random Road Disturbance Suspension Deflection at 60m/hr.

Figure 4.37 shows that contradict the displacement of the suspension deflection a passive with a NPID controller. In this case, the peak-to-peak value comparison of the NPID controller reduces the peak value from 4.5 m to 0.3 m in the positive peak direction. Where as in the negative peak value direction, the NPID controller shows a higher value reduction (6.5 to 0.3) by giving a response to the change of the suspension deflection based on the NPID controller gain.

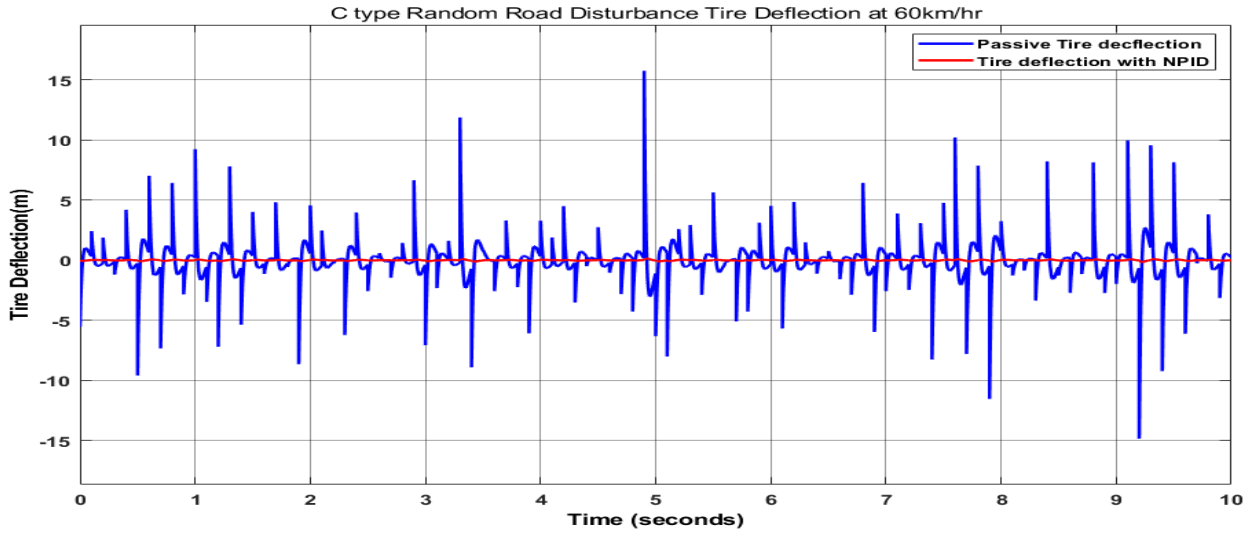


Figure 4.38 C type Random Road Disturbance Tire Deflection at 60km/hr.

Figure 4.38 shows that contradict the displacement of the chassis at the tire deflection passive with a NPID controller. In this case, the peak-to-peak value comparison of the NPID controller reduces the peak value from 16 m to 0.35 m in the positive peak direction. Whereas in the negative peak value direction, the NPID controller shows a higher value reduction (15 to 0.35m) by giving a response to the change of the tire deflection based on the NPID controller gain.

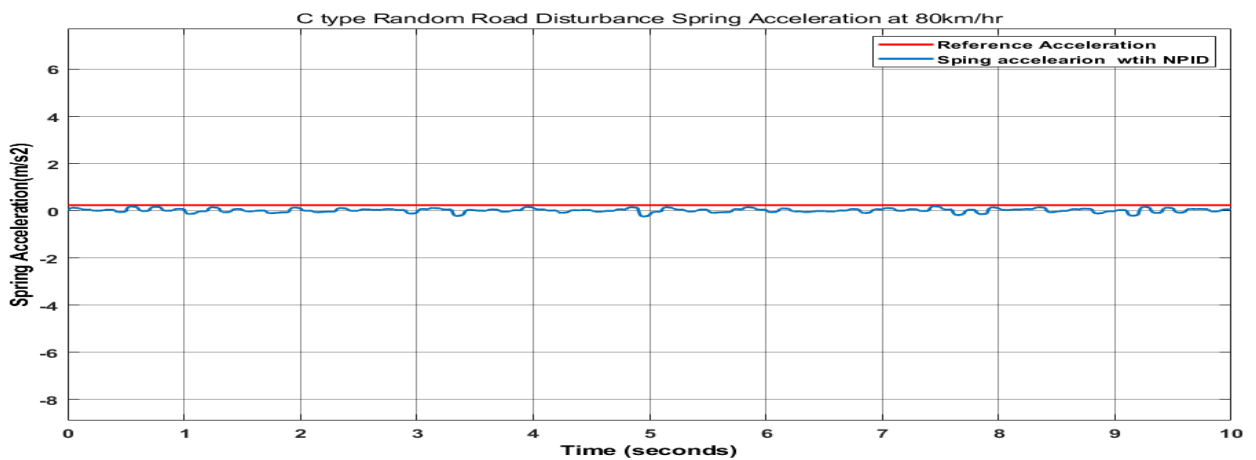


Figure 4.39 C type Random Road Disturbance Spring Acceleration at 80m/hr.

Figure 4.39 shows that contradict the reference acceleration with a NPID controller. In this case, the peak-to-peak value comparison of the NPID controller equal to the peak value from 0.2375 m to 0.2375 m in the positive peak direction. Whereas in the negative peak value

direction, the NPID controller shows a higher value reduction (0.23m) by giving a response to the change of the spring acceleration based on the NPID controller gain.

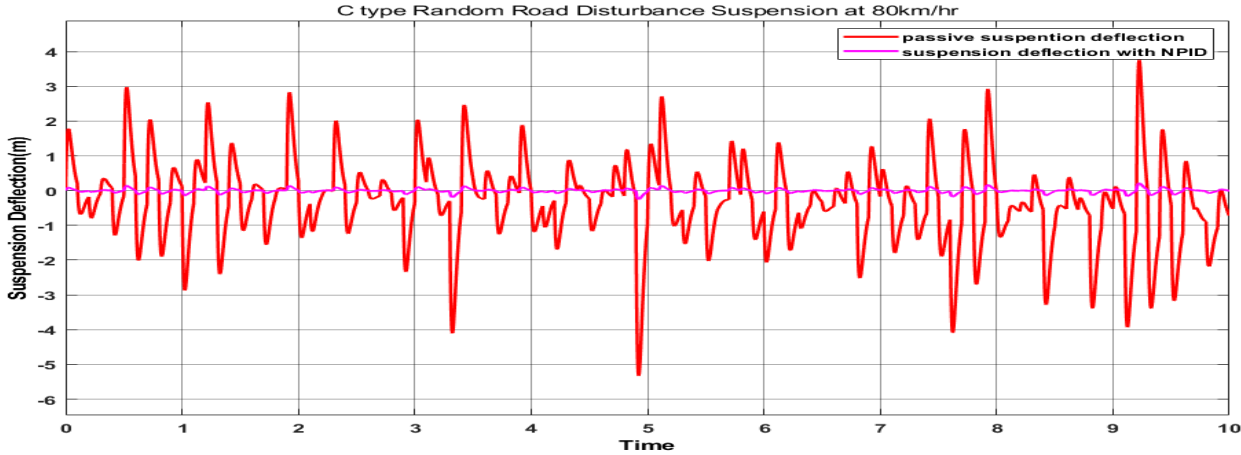


Figure 4.40 C type Random Road Disturbance Suspension Deflection at 80km/hr.

Figure 4.40 shows that contradict the displacement of the suspension deflection passive with a NPID controller. In this case, the peak-to-peak value comparison of the NPID controller reduces the peak value from 3.8 m to 0.25 m in the positive peak direction. Whereas in the negative peak value direction, the NPID controller shows a higher value reduction (5.4 to 0.25) by giving a response to the change of the suspension deflection based on the NPID controller gain.

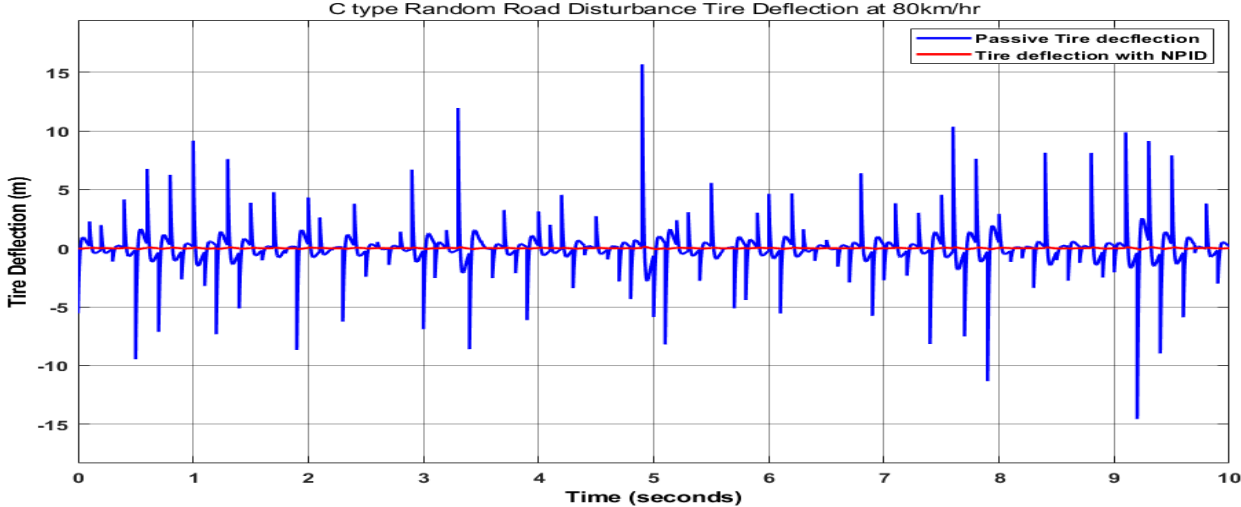


Figure 4.41 C type Random Road Disturbance Tire Deflection at 80km/hr.

Figure 4.41 shows that contradict the displacement of the tire deflection a passive with a NPID controller. In this case, the peak-to-peak value comparison of the NPID controller reduces the peak value from 15.75m to 0.3 m in the positive peak direction. Whereas in the negative peak value direction, the NPID controller shows a higher value reduction (14.9 to 0.3m) by giving a response to the change of the tire deflection based on the NPID controller gain.

Table 4.7: peak to peak values of PSS using type C random road input simulations

Parameters	Peak to peak PSS 20km/hr	Peak to peak PSS 40km/hr	Peak to Peak PSS 60km/hr	Peak to Peak PSS 80km/hr
Spring Acceleration (m/s ²)	0.2375	0.2375	0.2375	0.2375
Suspension Deflection(m)	15.5	12.9	11	9.2
Tire Deflection(m)	32.5	31.5	31	30.65

Table 4.8: peak to peak values of ASS using type C random road input simulations

Parameters	Peak to peak ASS 20km/hr	Peak to peak ASS 40km/hr	Peak to Peak ASS 60km/hr	Peak to Peak ASS 80km/hr
Spring Acceleration (m/s ²)	0.2375	0.2375	0.2375	0.237
Suspension Deflection(m)	0.6	0.6	0.6	0.6
Tire	0.6	0.7	0.7	0.6

Deflection(m)				
---------------	--	--	--	--

4.7 Summery

This thesis focuses on the performance analysis of suspension systems, specifically the 2DOF suspension model for a quarter car. The study compares active systems with passive systems, employing an active system with an NPID controller. The simulation results demonstrate that the suspension system with the controller effectively improves both objectives of the study. These objectives are:

Improved Ride Comfort: The active quarter car suspension system with a non-linear PID controller can significantly enhance ride comfort compared to passive suspension systems. The controller can actively adjust the suspension parameters based on real-time feedback, reducing the effect of road disturbances and providing a smoother ride for the passengers.

Enhanced Stability: The non-linear PID controller can improve the stability of the vehicle by adapting the suspension characteristics to different road conditions. It can dynamically adjust the damping forces and stiffness of the suspension, minimizing body roll, pitch, and other undesired motions during cornering, braking, and acceleration.

In the previous section, the analysis includes both expected and random road inputs, with road models developed for specific vehicle speeds. The simulation entails plotting various performance evaluation graphs using different road disturbance types (A, B, and C). Throughout these simulations, the effects of road profiles and vehicle speeds are observed in the dynamic model, specifically in terms of sprung mass vertical displacement and wheel displacement in the vertical direction. It becomes evident that driving the vehicle on rough road surfaces leads to higher discomfort compared to smooth road surfaces. Similarly, higher discomfort is experienced with high vehicle speeds and disturbance inputs compared to lower vehicle speeds. However, the newly designed model demonstrates remarkable improvements, even for high-speed vehicles on rough road surfaces. Each figure presents valuable insights into the vertical displacement of the vehicle body and the wheel, while also highlighting the control of the unsprung mass and the enhanced traction capability of the wheel.

CHAPTER FIVE

5 CONCLUSION AND RECOMMENDATION

5.1 Conclusion

This thesis work successfully implements NPID control techniques in a hydraulic actuator suspension system for a quarter car model. The primary objective of minimizing road disturbances in the quarter-car model is effectively achieved through the utilization of NPID controllers. The study demonstrates that an active suspension system, incorporating a non-linear actuator, provides additional design flexibility. By integrating the NPID controller with the actuator, the system significantly enhances ride quality and vehicle handling. Furthermore, the system exhibits full rank, indicating that it is fully controllable.

The implementation of a NPID controller in the new design effectively manages the dynamic effects of both expected and random road inputs. The Simulink graph confirms that the controller brings about improvements in both comfort and handling. Specifically, compared to an uncontrolled PSS (Passive Suspension System), the controlled ASS (Active Suspension System) exhibits reduced peak-to-peak displacement, settling time, spring acceleration, and tire deflection. This demonstrates the superior performance of the designed controller in enhancing ride comfort and road handling across various road disturbances and vehicle speeds.

As previously mentioned in the introduction, the evaluation of vehicle suspension system performance encompasses elements such as ride comfort, suspension travel, and road handling. Among these elements, prioritizing passenger comfort by minimizing passenger acceleration is of utmost importance. The result of the study further confirms that the new design successfully improves ride quality.

5.2 Recommendation

Across different road disturbances and vehicle speeds, the suspension system equipped with the controller proves to be highly effective in creating a dynamic model that enhances both ride comfort and road handling. It is worth noting that smoother road conditions and moderate vehicle speeds offer superior ride comfort and road handling compared to rough road surfaces

and high vehicle speeds. In light of these findings, the author recommends that interested academics focus on developing controllers for vehicle models to improve performance across various road profiles, including those with poor road conditions, as well as half and full car suspensions.

5.3 Future work

The objective of this thesis is to forecast the performance of an active suspension system by utilizing a quarter-car model. It is important to note that the quarter-car model represents a simplified version of the full automobile model, disregarding certain aspects of the vehicle's behavior, such as rolling and yaw. To attain optimal results in these domains as well, further exploration should be conducted using a more comprehensive model that encompasses these degrees of freedom

Research fund Acknowledgment

This research thesis was funded by Adama Science and Technology University under the grant number **ASTU/SM-R/819/23**, Adama, Ethiopia.

REFERENCE

- Abdullah, L., Jamaludin, Z., Ahsan, Q., Jamaludin, J., Rafan, N. A., Heng, C. T., Jusoff, K., & Yusoff, M. (2013). Evaluation on tracking performance of PID, gain scheduling and classical cascade P/PI controller on XY table ballscrew drive system. *World Applied Sciences Journal*, 21(SPECIAL ISSUE2), 1–10. <https://doi.org/10.5829/idosi.wasj.2013.21.1001>
- Ahmad, I., & Khan, A. (2018). A Comparative Analysis of Linear and Nonlinear Semi-Active Suspension System. *Mehran University Research Journal of Engineering and Technology*, 37(2), 233–240. <https://doi.org/10.22581/muet1982.1802.01>
- Ang, K. H., Chong, G., & Li, Y. (2005). PID control system analysis, design, and technology. *IEEE Transactions on Control Systems Technology*, 13(4), 559–576. <https://doi.org/10.1109/TCST.2005.847331>
- Ayele, B., Santhosh, J., Ahmed, A. A., & Ponnusamy, M. (2020). *Non-Linear Mathematical Modelling for Quarter Car Suspension Model*. November.
- Azizi, A., & Mobki, H. (2021). Applied Mechatronics: Designing a Sliding Mode Controller for Active Suspension System. *Complexity*, 2021. <https://doi.org/10.1155/2021/6626842>
- Greg Shinskey, F. (2017). PID control. *Measurement, Instrumentation, and Sensors Handbook: Spatial, Mechanical, Thermal, and Radiation Measurement, Second Edition*, 91-1-91–99. <https://doi.org/10.1201/b15474>
- Hunnekens, B. G. B., Heertjes, M. F., Van De Wouw, N., & Nijmeijer, H. (2014). Performance optimization of piecewise affine variable-gain controllers for linear motion systems. *Mechatronics*, 24(6), 648–660. <https://doi.org/10.1016/j.mechatronics.2014.02.011>
- I., S., Salim, S. I. M., Yusop, A. S., & Sulaiman, N. (2018). A comparative study of enhanced nonlinear PI to multivariable nonlinear plant. *Journal of Telecommunication, Electronic and Computer Engineering*, 10(2–7), 23–26.
- Meng, Q., Chen, C. C., Wang, P., Sun, Z. Y., & Li, B. (2021). Study on vehicle active suspension system control method based on homogeneous domination approach. *Asian*

Journal of Control, 23(1), 561–571. <https://doi.org/10.1002/asjc.2242>

Nagarkar, M., Bhalerao, Y., Patil, G. V., & Patil, R. Z. (2018). Multi-Objective Optimization of Nonlinear Quarter Car Suspension System - PID and LQR Control. *Procedia Manufacturing*, 20, 420–427. <https://doi.org/10.1016/j.promfg.2018.02.061>

Omar, M., El-kassaby, M. M., & Abdelghaffar, W. (2018). Parametric numerical study of electrohydraulic active suspension performance against passive suspension. *Alexandria Engineering Journal*, 57(4), 3609–3614. <https://doi.org/10.1016/j.aej.2018.05.007>

Shafiei, B. (2022). A Review on PID Control System Simulation of the Active Suspension System of a Quarter Car Model While Hitting Road Bumps. *Journal of The Institution of Engineers (India): Series C*, 103(4), 1001–1011. <https://doi.org/10.1007/s40032-022-00821-z>

Sharkawy, A., Ali, A. S., Ghazaly, N. M., & Abdel-jaber, G. (2015). *PID CONTROLLER OF ACTIVE SUSPENSION SYSTEM FOR A QUARTER CAR*. April 2016.

Taskin, Y., Yuksek, I., & Yagiz, N. (2017). Vibration control of vehicles with active tuned mass damper. *Journal of Vibroengineering*, 19(5), 3533–3541. <https://doi.org/10.21595/jve.2017.18138>

Wang, H. P., Mustafa, G. I. Y., & Tian, Y. (2018). Model-free fractional-order sliding mode control for an active vehicle suspension system. *Advances in Engineering Software*, 115(November), 452–461. <https://doi.org/10.1016/j.advengsoft.2017.11.001>

Wang, X. (2017). *Linear Extended State Observer-Based Motion Synchronization Control for Hybrid Actuation System of More Electric Aircraft*. <https://doi.org/10.3390/s17112444>

Youness, S. F., & Lobusov, E. C. (2019). Networked control for active suspension system. *Procedia Computer Science*, 150, 123–130. <https://doi.org/10.1016/j.procs.2019.02.025>

APPENDIXES

Table Acceleration level and Degree of comfort defined in ISO2631-1 [24-26]

Acceleration level	Degree of comfort
Less than 0.315 m/s ²	Not uncomfortable
0.315-0.63 m/s ²	A little uncomfortable
0.5-1 m/s ²	Fairly uncomfortable
0.8-1.6 m/s ²	Uncomfortable
1.25-2.5 m/s ²	Very uncomfortable
Greater than 2 m/s ²	Extremely uncomfortable

To obtain maximum gain value

% Define the system transfer function

S = tf('s');

$$G = (3.436 \cdot 10^6 \cdot S^4 + 2.393 \cdot 10^7 \cdot S^3 + 1.386 \cdot 10^9 \cdot S^2 + 9.366 \cdot 10^9 \cdot S + 1.618 \cdot 10^{10}) / (S^6 + 3946 \cdot S^5 + 7.826 \cdot 10^5 \cdot S^4 + 2.741 \cdot 10^7 \cdot S^3 + 1.907 \cdot 10^9 \cdot S^2 + 1.04 \cdot 10^{10} \cdot S + 2.045 \cdot 10^{10});$$

% Define the sector bound

error_min = 0;

error_max = 2;

alpha_min = 0;

alpha_max = 1;

% Define the Popov function

popov_func = @(error, alpha) (exp(alpha*error)+exp(-alpha*error)/2);

% Evaluate the Popov function over the sector bound

n_error = 10;

n_alpha = 10;

error_vals = logspace(log10(error_min), log10(error_max), n_error);

alpha_vals = linspace(alpha_min, alpha_max, n_alpha);

```

popov_vals = zeros(n_error, n_alpha);

for i = 1:n_error
    for j = 1:n_alpha
        popov_vals(i,j) = popov_func(error_vals(i), alpha_vals(j));
    end
end

% Find the maximum gain for Popov stability
popov_vals_reshaped = reshape (popov_vals, [], 1);
max_gain =max (sqrt (popov_vals_reshaped))

% Check if the system is stable
if max_gain < 3
    disp('System is stable by Popov stability criterion');
else
    disp('System is unstable by Popov stability criterion');
end

```

Tuned Non-linear proportional integral derivative value

P=6.22

I=0.228

D=1.31

Suspension deflection Values vary according to the type of car. For a small saloon the suspension deflection is often 110-140 mm, and the equivalent natural frequency between 90 and 80 cycles/mm. For a medium-size saloon, the suspension deflection is often 130-180 mm, between 85 and 70 cycles/mm; for a large saloon, 180-280 mm, between 70 and 55 cycles/mm. With some very advanced suspensions, suspension deflection of over 280 mm or under 55 cycles/mm are obtained.